JHEP

Published for SISSA by Springer

Received: December 13, 2018
Revised: April 18, 2019
Accepted: May 31, 2019
Published: June 10, 2019

Exotic Higgs decays in Type-II 2HDMs at the LHC and future 100 TeV hadron colliders

Felix Kling,[a] **Honglei Li,**[b] **Adarsh Pyarelal,**[c] **Huayang Song**[d] **and Shufang Su**[d]

[a] *Department of Physics and Astronomy, University of California, Irvine, CA 92697, U.S.A.*
[b] *School of Physics and Technology, University of Jinan, Jinan Shandong 250022, China*
[c] *School of Information, University of Arizona, Tucson, Arizona 85721, U.S.A.*
[d] *Department of Physics, University of Arizona, Tucson, Arizona 85721, U.S.A.*

E-mail: fkling@uci.edu, sps_lihl@ujn.edu.cn, adarsh@email.arizona.edu, huayangs@email.arizona.edu, shufang@email.arizona.edu

Abstract: The exotic decay modes of non-Standard Model (SM) Higgses in models with extended Higgs sectors have the potential to serve as powerful search channels to explore the space of Two-Higgs Doublet Models (2HDMs). Once kinematically allowed, heavy Higgses could decay into pairs of light non-SM Higgses, or a non-SM Higgs and a SM gauge boson, with branching fractions that quickly dominate those of the conventional decay modes to SM particles. In this study, we focus on the prospects of probing Type-II 2HDMs at the LHC and a future 100 TeV pp collider via exotic decay channels. We study the three prominent exotic decay channels: $A \to HZ$, $A \to H^{\pm}W^{\mp}$ and $H^{\pm} \to HW^{\pm}$, and find that a 100-TeV pp collider can probe most of the region of the Type-II 2HDM parameter space that survives current theoretical and experimental constraints with sizable exotic decay branching fraction through these channels, making them complementary to the conventional decay channels for heavy non-SM Higgses.

Keywords: Beyond Standard Model, Higgs Physics

ArXiv ePrint: 1812.01633

https://doi.org/10.1007/JHEP06(2019)031

JHEP06(2019)031

Contents

1 Introduction **1**

2 Hierarchical Two Higgs Doublet Models: a review **3**
- 2.1 Properties of 2HDMs 3
- 2.2 Couplings in the alignment limit 4
- 2.3 Constraints on hierarchical 2HDMs 5
- 2.4 Exotic Higgs decays in hierarchical 2HDMs 7
- 2.5 Production cross sections 8
- 2.6 Prospects for conventional Higgs search channels 10

3 The neutral Higgs channel: $A \to HZ$ **11**
- 3.1 Signal processes 11
- 3.2 Analysis 12
- 3.3 Reach 14

4 The charged Higgs channel: $A \to H^{\pm}W^{\mp}$ **16**
- 4.1 Signal processes 16
- 4.2 Analysis 16
- 4.3 Reach 17

5 Exotic charged Higgs decays: $H^{\pm} \to HW^{\pm}$ **18**
- 5.1 Signal processes 18
- 5.2 Analysis 18
- 5.3 Reach 19

6 Reach in benchmark planes **19**

7 Conclusion **22**

A Collider analysis methodology **24**

B Simulation of top-tagging **26**

1 Introduction

With the discovery of a light Standard Model (SM)-like Higgs boson at the LHC [1, 2], the search for new physics beyond the SM has become even more pressing, given the need to stabilize the mass of the Higgs boson against large radiative corrections. Many of the new physics models constructed to augment the SM contain an extended Higgs sector that is

JHEP06(2019)031

responsible for electroweak symmetry breaking. One of the most straightforward and well-motivated class of extensions to the SM is the category of models collectively known as Two-Higgs-Doublet Models (2HDMs) [3]. After electroweak symmetry breaking, the spectra of 2HDMs (minimally) contain five mass eigenstates (h, H, A, $H^{\pm}$), with the CP-even Higgs h being the observed SM-like Higgs. These new Higgs bosons can be constrained through either indirect searches via precision measurements of Higgs properties at future Higgs factories [4, 5] or direct searches at particle colliders at the energy frontier. In this paper, we focus on the latter scenario, in particular the potential for direct discovery of these heavy states at the Large Hadron Collider (LHC) as well as a proposed 100 TeV pp collider [6, 7].

The conventional searches for heavy Higgses in 2HDMs mainly focus on modes in which they decay into pairs of SM particles. However, if the beyond-the-SM (BSM) Higgs sector is *hierarchical* — that is, its states are sufficiently well-separated in mass — additional decay channels open up, e.g., the decay of a heavy Higgs to two lighter Higgses, or to a lighter Higgs and a SM gauge boson. Given the corresponding unsuppressed couplings and the large amount of available phase space, these decay modes can be dominant in large regions of parameter space. In such a scenario, the branching fractions of the conventional decay modes are reduced and the experimental search limits obtained using them correspondingly relaxed [8–12].

The *exotic* decay modes of heavy Higgses to lighter Higgses and vector bosons, namely $H \to AZ/H^{\pm}W^{\mp}$, $A \to hZ/HZ/H^{\pm}W^{\mp}$ and $H^{\pm} \to hW/HW/AW$, as well as to two lighter Higgses, $H \to AA/hh/H^{+}H^{-}$, offer alternative avenues for discovering heavy Higgses that complement the conventional ones. The reaches of individual channels at the LHC have been studied in the literature [8–11] and searches for the most promising channel, $H/A \to AZ/HZ$, have been carried out at both ATLAS [13] and CMS [14]. The current experimental data exclude heavy neutral Higgses with masses up to about 700–800 GeV, depending on the BSM Higgs spectrum and values of $\tan\beta$. Additionally, the $A \to hZ$, $H \to hh$ channels have also been studied at the LHC [15–17]. However, no constraints on the parameter space of 2HDMs can be imposed using these channels. This is because the observed Higgs boson is SM-like, corresponding to the alignment limit in 2HDMs, in which such channels are highly suppressed.

The study in ref. [12] constructs benchmark planes for these exotic decay channels at the LHC, taking into account both theoretical constraints such as perturbativity, unitarity, and vacuum stability, as well as current experimental limits from direct and indirect searches on the parameter space of Type-II 2HDMs. Sizable mass splittings between Higgses, required for the exotic decay modes, can be achieved for heavy Higgs masses up to about 2 TeV. Thus, in this paper, we focus on a subset of the benchmark scenarios in ref. [12] that permit TeV-scale masses, and construct two benchmark planes: **BP-A** ($m_A > m_H = m_{H^{\pm}}$) with $A \to HZ/H^{\pm}W^{\mp}$ and **BP-B** ($m_A = m_{H^{\pm}} > m_H$) with $A \to HZ$, $H^{\pm} \to HW^{\pm}$.

In recent years, a possible 100 TeV pp collider has been discussed worldwide, with the two leading proposals being the Future Circular Collider (FCC) at CERN [7, 18] and the Super proton-proton Collider (SppC) in China [6]. It is important to explore the discovery potential for new physics models at such a machine to establish the physics case for building

JHEP06(2019)031

it. One advantage of such a high energy machine is that top quarks produced in heavy particle decays will be highly boosted, resulting in fat jets that can be effectively identified using top-tagging techniques [19–24]. This will allow us to distinguish new physics signals with top quarks in the final states from the large SM backgrounds involving top quarks, which typically pose a formidable challenge at the LHC.

In this paper, we study the discovery potential of non-SM heavy Higgses in Type-II 2HDMs at the LHC, the High Luminosity LHC (HL-LHC), as well as a 100 TeV pp collider:

$$\textbf{LHC: } \mathcal{L} = 300\,\text{fb}^{-1}, \quad \textbf{HL-LHC: } \mathcal{L} = 3\,\text{ab}^{-1}, \quad \textbf{100 TeV: } \mathcal{L} = 3\,\text{ab}^{-1}, \tag{1.1}$$

combining all the viable exotic decay channels. We perform a detailed collider analysis to obtain the 95% C.L. exclusion limits as well as 5σ discovery reach for benchmark planes **BP-A** and **BP-B**. In recent years, multivariate analysis techniques such as neural networks [1], boosted decision trees (BDT) [2], the Matrix Element Method [25, 26] and Information Geometry [27, 28] have begun to be more widely used in experimental particle physics searches. In our study, we construct a set of physics-motivated variables that we use as input features for gradient BDT classifiers.

The rest of the paper is organized as follows. In section 2, we present a brief review of hierarchical 2HDMs and introduce the benchmark planes **BP-A** and **BP-B**. We also discuss the prospects of the conventional Higgs search channels. In section 3, we study the channels $A/H \to HZ/AZ$ and explore their reach at the LHC, HL-LHC, as well as a 100 TeV pp collider. In particular, we study both the $bb\ell\ell$ and $\tau\tau\ell\ell$ states as well as the $tt\ell\ell$ final state using top tagging techniques to identify boosted top quarks in the final state. In section 4, we present the analysis for the $H \to H^{\pm}W^{\mp}$ channel. In section 5, we explore the discovery potential for charged Higgses via the $H^{\pm} \to HW^{\pm}$ channel. In section 6, we present the combined reach in 2HDM parameter space obtained with these channels at the LHC and a future 100 TeV pp collider. In section 7, we conclude. Appendix A and appendix B describe the methodology used for our collider analysis and top tagging simulation, respectively.

2 Hierarchical Two Higgs Doublet Models: a review

2.1 Properties of 2HDMs

In this section, we provide a brief review of the aspects of 2HDMs that are most relevant to this study. For pedagogical introductions to this topic, see [29, 30]. The scalar sector of 2HDMs consists of two SU(2) doublets Φ_i, with $i = 1, 2$, which can be explicitly parameterized in terms of their real and complex components as shown below.

$$\Phi_i = \begin{pmatrix} \phi_i^+ \\ (v_i + \phi_i + i\varphi_i)/\sqrt{2} \end{pmatrix} \tag{2.1}$$

Here, v_i are the vacuum expectation values (VEVs) for the neutral components of the doublets, that satisfy the condition $v_1^2 + v_2^2 = v^2$, with $v = 246\,\text{GeV}$. This allows us to

JHEP06(2019)031

introduce the mixing angle β such that $\tan\beta = v_2/v_1$.[1] The most general scalar potential also contains the term $\left[\lambda_6(\Phi_1^\dagger\Phi_1) + \lambda_7(\Phi_2^\dagger\Phi_2)\right](\Phi_1^\dagger\Phi_2) + h.c.$ and potentially leads to flavor-changing neutral currents (FCNCs). In the following we will neglect this term by imposing a $\mathcal{Z}_2$ symmetry under which the scalar fields transform as $\Phi_1 \to -\Phi_1$ and $\Phi_2 \to \Phi_2$. Assuming CP conservation and a softly-broken $\mathcal{Z}_2$ symmetry, the scalar portion of the 2HDM Lagrangian can be written down as

$$\begin{aligned} V(\Phi_1,\Phi_2) = {} & m_{11}^2\Phi_1^\dagger\Phi_1 + m_{22}^2\Phi_2^\dagger\Phi_2 - m_{12}^2(\Phi_1^\dagger\Phi_2 + h.c.) + \frac{\lambda_1}{2}(\Phi_1^\dagger\Phi_1)^2 + \frac{\lambda_2}{2}(\Phi_2^\dagger\Phi_2)^2 \\ & + \lambda_3(\Phi_1^\dagger\Phi_1)(\Phi_2^\dagger\Phi_2) + \lambda_4(\Phi_1^\dagger\Phi_2)(\Phi_2^\dagger\Phi_1) + \frac{1}{2}\left[\lambda_5(\Phi_1^\dagger\Phi_2)^2 + h.c.\right]. \end{aligned} \tag{2.2}$$

After the mechanism of electroweak symmetry breaking (EWSB), the scalar sector of a 2HDM consists of five mass eigenstates: a pair of neutral CP-even Higgses, h and H, a CP-odd Higgs, A, and a pair of charged Higgses $H^\pm$. For these states we can write

$$\begin{aligned} h &= -s_\alpha\,\phi_1 + c_\alpha\,\phi_2, & A &= -s_\beta\,\varphi_1 + c_\beta\,\varphi_2, \\ H &= \;\; c_\alpha\,\phi_1 + s_\alpha\,\phi_2, & H^\pm &= -s_\beta\,\phi_1^\pm + c_\beta\,\phi_2^\pm. \end{aligned} \tag{2.3}$$

In the following, we will identify h with the discovered SM-like 125 GeV Higgs[2] and study the collider reach of heavy non-SM Higgses.

The potential in eq. (2.2) contains eight independent parameters: three mass parameters $m_{11,22,12}^2$ and five quartic couplings $\lambda_{1,2,3,4,5}$. For our purposes, it is convenient to parameterize 2HDMs by the physical Higgs masses, m_h, m_H, m_A and $m_{H^\pm}$, the mixing angle between the two CP-even Higgses α, $\tan\beta$, the electroweak VEV v, and the soft $\mathcal{Z}_2$ symmetry breaking parameter m_{12}^2. Two of these parameters, namely the vacuum expectation value v and the mass of the SM-like Higgs, m_h are known to be 246 GeV and 125 GeV respectively, leaving the remaining six independent parameters. Note that in a generic 2HDM, there are no mass relations between the Higgs states, and therefore exotic Higgs decays such as $A \to HZ$ are possible.

As mentioned earlier, we have introduced a $\mathcal{Z}_2$ symmetry to avoid tree-level FCNCs, which implies that each fermion type is only allowed to couple to one Higgs doublet. In this work we will focus on Type-II 2HDMs, in which the up-type quarks only couple to Φ_2, and the down-type quarks and leptons only couple to Φ_1.

2.2 Couplings in the alignment limit

The most recent data from the LHC indicate that the coupling strength of the recently discovered 125 GeV Higgs boson is consistent with the SM [32]. In the context of a 2HDM, this can naturally be achieved in the *alignment limit*, where $c_{\beta-\alpha} = 0$, with h being

[1] In this paper we often employ the shorthand notation $s_\theta, c_\theta, t_\theta = \sin\theta, \cos\theta, \tan\theta$.

[2] This is slightly different from the usual convention that the mass eigenstates h^0 and H^0 are ordered by their masses. In this study, h can either be the light one or the heavy one. In our discussion of the collider study below, which focusses on heavy BSM Higgs boson, H is typically taken to be the heavy CP-even Higgs, although H being the light CP-even Higgs is still viable given the current experimental search results [31].

JHEP06(2019)031

identified with the SM Higgs in our convention. Its couplings to fermions and gauge bosons are precisely those predicted by the SM.

Any deviation of the signal strength of the SM-like Higgs h from its SM prediction will constitute clear evidence for new physics and provide strong motivation for additional experimental searches to understand its nature. In the absence of such deviations at the LHC, or possibly a future lepton collider, future limits will further push us towards the alignment limit [4, 5, 8]. For this reason, the following discussion will assume $c_{\beta-\alpha} = 0$. A discussion of the more general case can be found in [12].

Near the alignment limit, the coupling of the SM-like Higgs h to pairs of gauge bosons $V = Z, W^\pm$ is SM-like, while the coupling of the heavier CP-even neutral Higgs H to gauge boson pairs is suppressed, $g_{HVV} \sim c_{\beta-\alpha}$. Furthermore, the couplings of h to a heavier scalar and a gauge boson $g_{hAZ} \sim g_{hH^\pm W^\mp} \sim c_{\beta-\alpha}$ are also suppressed. The unsuppressed[3] couplings of the additional scalars to vector bosons in the alignment limit are given by

$$g_{HAZ} = \frac{m_Z}{v}(p_H^\mu - p_A^\mu),\ g_{HH^\pm W^\mp} = \pm\frac{im_W}{v}(p_H^\mu - p_{H^\pm}^\mu),\ g_{AH^\pm W^\mp} = \frac{m_W}{v}(p_{H^\pm}^\mu - p_A^\mu), \quad (2.4)$$

where p_X^μ represents the outgoing momentum for particle X. We can see that the non-SM like Higgses have unsuppressed couplings only to the other non-SM like Higgses, but suppressed couplings to the SM-like Higgs and pairs of gauge bosons. Therefore, only the heavier non-SM Higgs will decay into a lighter non-SM like Higgs and a gauge boson via an exotic decay mode. The lightest non-SM like Higgs will then decay into fermion pairs. In a Type-II 2HDM, the couplings of the non-SM Higgses to SM fermion pairs in the alignment limit can be written as

$$g_{Huu} = -g_{Auu}\gamma^5 = y_u t_\beta^{-1}, \quad g_{Hdd} = g_{Add}\gamma^5 = -y_d t_\beta, \quad g_{H\ell\ell} = g_{A\ell\ell}\gamma^5 = -y_\ell t_\beta, \quad (2.5)$$

where y_f are the SM fermion Yukawa couplings. Note that the fermion coupling for both heavy neutral scalars, A and H, have the same scaling with the mixing angle β under the alignment limit. The couplings of the charged Higgs boson to the fermions are

$$g_{H^\pm u_i d_j} = \frac{V_{ij}}{\sqrt{2}}\left[(t_\beta y_d + t_\beta^{-1} y_u) + (t_\beta y_d - t_\beta^{-1} y_u)\gamma^5\right], \qquad g_{H^\pm \ell\nu} = \frac{t_\beta y_\ell}{\sqrt{2}}(1+\gamma^5)\ . \quad (2.6)$$

2.3 Constraints on hierarchical 2HDMs

To understand the theoretical constraints on 2HDMs, it is useful to consider the relations between the quartic couplings and the physical masses. In the alignment limit, we can express the quartic couplings of the scalar potential as follows [12].

$$\begin{aligned}
v^2\lambda_1 &= m_h^2 - t_\beta^2\left[\frac{m_{12}^2}{s_\beta c_\beta} - m_H^2\right], \qquad v^2\lambda_4 = m_A^2 - 2m_{H^\pm}^2 + m_H^2 + \left[\frac{m_{12}^2}{s_\beta c_\beta} - m_H^2\right], \\
v^2\lambda_2 &= m_h^2 - t_\beta^{-2}\left[\frac{m_{12}^2}{s_\beta c_\beta} - m_H^2\right], \qquad v^2\lambda_5 = m_H^2 - m_A^2 + \left[\frac{m_{12}^2}{s_\beta c_\beta} - m_H^2\right], \\
v^2\lambda_3 &= m_h^2 + 2m_{H^\pm}^2 - 2m_H^2 - \left[\frac{m_{12}^2}{s_\beta c_\beta} - m_H^2\right].
\end{aligned} \quad (2.7)$$

[3] Note that the couplings of two CP-even or CP-odd Higgses to the Z-boson, as well as the coupling of two Z-bosons and a CP-odd Higgs, vanish since such a coupling would violate CP-invariance. A coupling of the charged scalar $H^\pm$ to a pair of vector bosons at most appears at loop level.

JHEP06(2019)031

We can see that the soft $\mathcal{Z}_2$ breaking term m_{12}^2 plays a crucial role, as it affects the size of the trilinear and quartic scalar self-couplings. As discussed in [12], its possible allowed values are dictated by requiring vacuum stability and tree-level unitarity of the theory. The latter roughly requires the quartic couplings to be perturbative, $\lambda_i \lesssim 4\pi$. Thus, perturbativity of $\lambda_{1,2}$ requires $|m_{12}^2 - m_H^2 s_\beta c_\beta| \lesssim v^2$, which naturally leads us to fix the coefficient of the soft $\mathcal{Z}_2$ breaking term in the Lagrangian to be

$$m_{12}^2 = m_H^2 s_\beta c_\beta. \tag{2.8}$$

It is possible to deviate from this relation for values of t_β close to unity and for low scalar masses $m_H \sim v$. However, in this study we focus on the high scalar mass region that can be probed at a future high energy collider and we therefore require eq. (2.8) to hold for the rest of the paper.

In the following, we summarize the theoretical and experimental constraints on the parameter space of 2HDMs, and their implications for exotic Higgs decays. We only consider the alignment limit $c_{\beta-\alpha} = 0$ and require $m_{12}^2 = m_H^2 s_\beta c_\beta$. A more detailed discussion is presented in [12].

Vacuum stability. In order to have a stable electroweak vacuum [33], the following scalar mass conditions need to be fulfilled:

$$m_h^2 + m_{H^\pm}^2 - m_H^2 > 0, \quad \text{and} \quad m_h^2 + m_A^2 - m_H^2 > 0\,. \tag{2.9}$$

This implies that for $m_H > m_{A,H^\pm}$, the mass splittings between the heavy CP-even Higgs H and the other heavy scalars A and $H^\pm$ have to be small, such that the decays of H into the AZ, AA, H^+H^- and $H^\pm W^\mp$ final states are not kinematically allowed.

Tree-level unitarity. Requiring tree-level unitarity of the scattering matrix in the 2HDM scalar sector [34] imposes the following additional mass constraints:

$$\begin{aligned} &|m_H^2 - m_A^2| < 8\pi v^2, \quad |3m_H^2 + m_A^2 - 4m_{H^\pm}^2| < 8\pi v^2, \quad |m_H^2 + m_A^2 - 2m_{H^\pm}^2| < 8\pi v^2, \\ &|3m_H^2 - m_A^2 - 2m_{H^\pm}^2| < 8\pi v^2, \quad |3m_H^2 - 5m_A^2 + 2m_{H^\pm}^2| < 8\pi v^2. \end{aligned} \tag{2.10}$$

Here we have ignored sub-leading terms proportional to m_h^2. Note that these constraints are independent of the value of t_β.

Electroweak precision measurements. Measurements of electroweak precision observables impose strong constraints on the 2HDM mass spectrum [35]. In particular, these constraints require the charged scalar mass to be close to the mass of one of the heavy neutral scalars.

$$m_{H^\pm} \approx m_H \quad \text{or} \quad m_{H^\pm} \approx m_A. \tag{2.11}$$

Flavour constraints. Various flavor measurements [35, 36] provide indirect constraints on the 2HDM parameter space, in particular on the mass of the charged scalar. The most stringent of these comes from the measurement of the branching fraction for the decays $b \to s\gamma$ and $B^+ \to \tau\nu$, which disfavor $m_{H^\pm} < 580\,\text{GeV}$ [37] and large values

JHEP06(2019)031

of t_β respectively. Flavor constraints, however, can be alleviated with contributions from other sectors of new physics models [38]. In this paper, we focus on the direct collider reach of heavy Higgses without imposing the flavor constraints.

Direct searches at LEP and LHC. While the search for pair-produced charged Higgs bosons at the Large Electron-Positron Collider (LEP) imposes a lower bound of 80 GeV on the mass of the charged Higgs boson [39], LEP searches for AH production constrain the sum of the masses $m_H + m_A > 209\,\text{GeV}$ [40]. LEP bounds on single neutral Higgs production do not apply in the alignment limit, due to their vanishing coupling to the gauge bosons. Note that limits from searches for conventional decays are significantly weakened once exotic Higgs decay channels are kinematically allowed. The ATLAS [13] and CMS [14] searches for the exotic decay mode $A/H \to HZ/AZ$ constrain hierarchical 2HDMs with low scalar masses.

Additional constraints for charged Higgs bosons are derived from experimental searches at the LHC via the $H^\pm \to \tau\nu$ decay mode. A light charged scalar with $m_{H^\pm} < m_t$ is mostly excluded by the non-observation of the decay $t \to H^+ b$, although these limits can be weakened at low t_β by the existence of exotic decay modes [11]. A heavy charged scalar is only weakly constrained at very large t_β [41–43]. For a detailed discussion of constraints on the charged Higgs, see [44].

2.4 Exotic Higgs decays in hierarchical 2HDMs

We have seen that in a 2HDM with heavy scalar masses close to the aligment limit, the requirements of unitarity and vacuum stability fix the soft $\mathcal{Z}_2$ breaking term $m_{12}^2 = m_H^2 s_\beta c_\beta$ and demand the mass hierarchy $m_H \leq m_A, m_{H^\pm}$. Additionally, electroweak precision constraints require the mass of the charged scalar to be close to that of one of the neutral scalars, $m_{H^\pm} \approx m_H$ or $m_{H^\pm} \approx m_A$. Hierarchical 2HDMs are therefore restricted to be close to the following two benchmark scenarios:

BP-A: $m_A > m_H = m_{H^\pm}$

If the charged Higgs $H^\pm$ is mass-degenerate with the heavy CP-even Higgs H, only the exotic decays of the pseudoscalar A are allowed ($A \to H^\pm W^\mp / HZ$). Requiring unitarity additionally imposes an upper bound on the mass splitting: $5(m_A^2 - m_H^2) < 8\pi v^2$.

BP-B: $m_A = m_{H^\pm} > m_H$

If the charged Higgs $H^\pm$ is mass-degenerate with the pseudoscalar A, only the exotic decays into the CP-even Higgs H are allowed: $H^\pm \to HW^\pm$ and $A \to HZ$. In this case, unitarity imposes an upper bound on the mass splitting: $3(m_A^2 - m_H^2) < 8\pi v^2$.

While these benchmark scenarios are representative, small deviations from them are permitted. This is illustrated in figure 1, where we show the accessible regions of the Type-II 2HDM parameter space in the alignment limit when all the theoretical considerations and precision constraints are taken into account. Note that these results are independent of the value of t_β.

JHEP06(2019)031

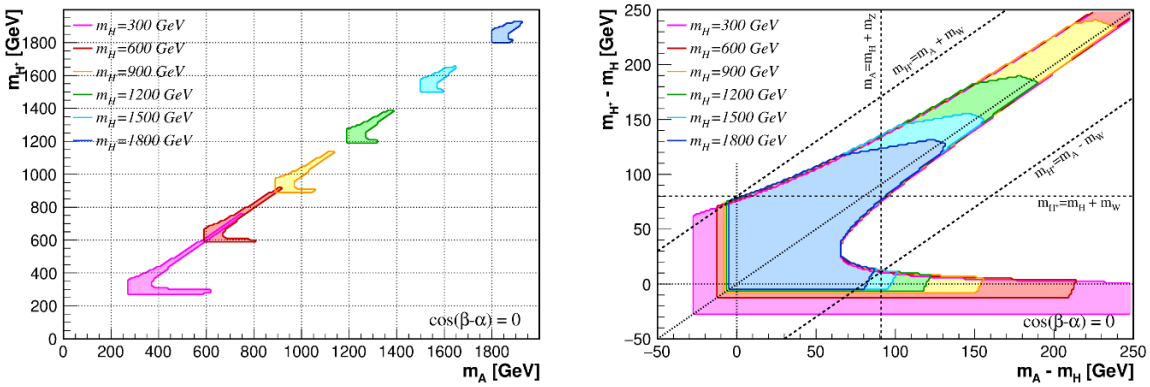

Figure 1. Allowed regions in parameter space of m_A vs. $m_{H^\pm}$ (left panel) and zoomed-in regions of $m_A - m_H$ vs. $m_{H^\pm} - m_H$ (right panel) considering electroweak constraints, unitarity and vacuum stability for different values of m_H. Here we consider the case with $c_{\beta-\alpha} = 0$ and $m_{12}^2 = m_H^2 s_\beta c_\beta$.

While the requirement of vacuum stability imposes a lower bound of m_H on m_A and $m_{H^\pm}$, electroweak precision constraints force the charged scalar to be almost mass degenerate with one of the neutral scalars. The additional unitarity constraints restrict the mass splittings, in particular for large scalar masses, to be small. This imposes an upper limit on the scalar masses in hierarchical 2HDMs that permit exotic Higgs decays. The exotic decay channel $A \to HZ$ becomes kinematically disallowed at $m_A \approx 1.7\,\text{TeV}$ for **BP-A** and $m_A \approx 2.8\,\text{TeV}$ for **BP-B**. Scalar particles in this mass range will be copiously produced at a future 100 TeV pp collider. Such a machine will therefore allow us to probe the *entire* hierarchical 2HDM parameter space, in which the heavy scalar predominantly decays via exotic modes. For even higher masses, the mass spectrum is forced to be near degenerate and can be effectively probed by conventional decay channels. Note that close to the alignment limit, exotic decays of the heavy Higgses into the light SM-like Higgs h, such as $A \to hZ$, $H \to hh$ and $H^\pm \to hW^\pm$, are suppressed by $c_{\beta-\alpha}$.

2.5 Production cross sections

In figure 2, we show the production cross sections of the CP-even (left panel), CP-odd (center panel), and charged (right panel) Higgs bosons at a 100 TeV pp collider as functions of their masses and t_β in the alignment limit. The dominant production processes for the neutral Higgses are gluon fusion ($gg \to A/H$) and bottom quark fusion ($bb \to A/H$), shown as solid red and dashed blue lines, respectively. The NNLO cross sections for both processes have been calculated using SusHi [45–47]. The gluon fusion process will be dominant in the small t_β region, where the production cross section can be greater than 10^5 fb for Higgs masses below 600 GeV. In contrast, the bottom-quark fusion process is dominant in the large t_β region. The charged Higgs is predominantly produced via the process $gg \to tbH^\pm$, and its production cross section has been adopted from ref. [48] (which used Prospino [49, 50] to calculate it).

JHEP06(2019)031

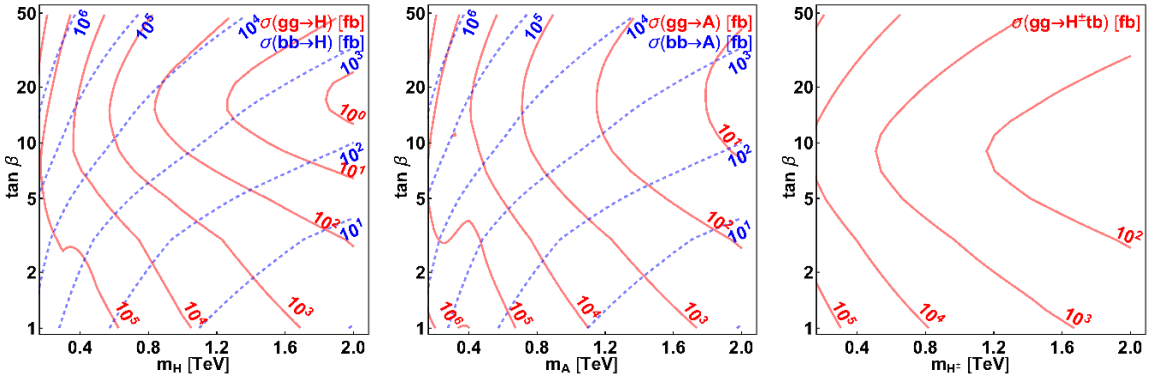

Figure 2. Production cross sections for the heavy Higgs bosons H (left), A (center) and $H^\pm$ (right) in a Type-II 2HDM in the alignment limit at a 100 TeV pp collider. The red and blue contours correspond to a gluon initial state and a bottom-quark initial state respectively.

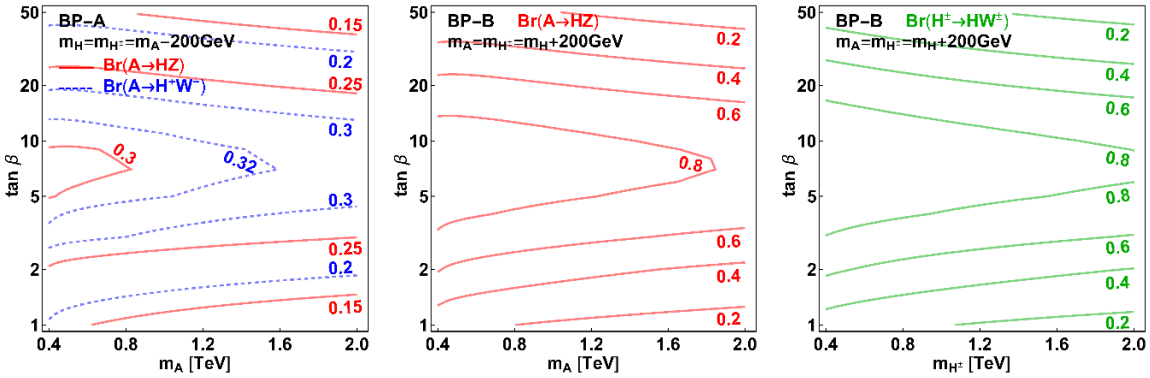

Figure 3. Branching fractions for the exotic Higgs decays $A \to HZ$ (red), $A \to H^+W^-$ (blue) and $H^\pm \to HW^\pm$ (green). Here we consider the benchmark points **BP-A** (left) and **BP-B** (center and right) with a mass splitting between the heavy Higgs bosons of $\Delta m = 200\,\text{GeV}$.

Compared to the 14 TeV LHC [12], a 100 TeV pp collider enhances the production rates of 500 GeV neutral Higgses by roughly a factor of 30–50. For charged Higgses with the same mass, the rate is enhanced by a factor of 90. For heavier Higgses, the enhancement is even greater.

In figure 3, we show the exotic branching fractions of heavy Higgs bosons as functions of their masses and t_β for the two benchmark scenarios defined in section 2.4. The exotic decay channels have sizable branching fractions ($\gtrsim 20$ %) over the entire parameter space and even dominate in the so-called *wedge* region, corresponding to moderate values of t_β ($2 \lesssim t_\beta \lesssim 20$). This phenomenon reduces the reach of the conventional search channels, but also opens up promising avenues for heavy Higgs searches in the form of the exotic decay channels. In particular, with the cleanness of the leptonic decay modes of the vector bosons, the exotic decays of heavy Higgses provide an opportunity to study the wedge region in 2HDMs.

JHEP06(2019)031

2.6 Prospects for conventional Higgs search channels

While searches for exotic decays can be powerful tools to probe hierarchical 2HDMs, there is also an established menu of conventional heavy Higgs search channels with heavy Higgses decaying to two SM fermions or gauge bosons. In the following, we summarize the current and proposed conventional searches for heavy Higgs bosons and discuss their expected performance (or lack thereof) in the context of the defined benchmark scenarios for hierarchical 2HDMs.

Searches probing the heavy neutral Higgs coupling to vector bosons. Searches for neutral Higgs bosons utilizing their coupling to vector bosons played an important role in the discovery of the SM-like Higgs boson. However, as we mentioned above, current data indicates that the properties of the observed 125 GeV Higgs are consistent with the SM, and therefore favoring the alignment limit $c_{\beta-\alpha} \approx 0$. This implies that the couplings of H to the SM weak gauge bosons are suppressed by $g_{HVV} \sim c_{\beta-\alpha}$, resulting in the suppression of their production via the weak-boson fusion and weak-boson associated processes, as well as their decays to SM gauge boson pairs $H \to WW/ZZ$.

Searches probing the heavy neutral Higgs coupling to b and τ. Due to the enhanced couplings at high $\tan\beta$ in Type-II 2HDMs, the $H \to bb$ and $H \to \tau\tau$ channels are two other channels that are frequently studied. In particular, the $H \to \tau\tau$ channel suffers less from complicated QCD backgrounds, becoming one of the most promising channels. The leading LHC bounds on neutral scalars come from searches for their conventional decays into pairs of τ-leptons [51, 52], and mainly constrain the low mass, high t_β region. Heavy neutral Higgses with $m_{A/H} \sim 300$–500 GeV are excluded for $\tan\beta \sim 10$, and up to about 1500 GeV for $\tan\beta \sim 50$. However, the sensitivity of these channels is reduced in the presence of exotic channels, and care must be taken while re-casting the experimental results.

Searches probing the heavy neutral Higgs coupling to tops. The dominant conventional decay mode of heavy neutral Higgs bosons H and A in the low $\tan\beta$ region is into a pair of top quarks. In this regime, the dominant production channel for heavy Higgs bosons is gluon fusion. However, it is known that the signal in the channel $gg \to H/A \to tt$ has strong interference effects with the SM tt background [53–55], resulting in a peak-dip structure in the tt invariant mass distribution. The ATLAS experiment has studied such signatures, constraining $m_{A/H}$ to around 500–600 GeV for $\tan\beta \lesssim 1$ in the alignment limit [56]. Projections for the HL-LHC [55] show that little gain is expected at higher luminosities.

While resonant heavy production in gluon fusion is unsatisfactory due to interference with the SM, searches using additional subdominant heavy Higgs production channels have been shown to be sensitive in this region. A search for heavy Higgses produced in association with one and two top quarks, $tW(H/A)$ and $tt(H/A)$, with subsequent decays into top pairs can utilize the same-sign dilepton signature to suppress backgrounds [57]. Similarly, the $bb(H/A)$ associated production channel with the subsequent decay $H/A \to tt$ shows promise in the wedge region ($\tan\beta \simeq 3$–10) [58].

JHEP06(2019)031

Searches for charged Higgs bosons. Due to their low production cross section, charged Higgs bosons pose a special challenge for experimental searches at the LHC [41–43]. They are dominantly produced in association with top quarks, $gg \to tbH^{\pm}$, with a cross section much smaller than that of the dominant production channels for the neutral Higgses. At high $\tan\beta$, the $H^{\pm} \to \tau\nu$ channel is dominant, and charged Higges with masses up to 1 TeV have been excluded for $\tan\beta \sim 60$ [42]. Projections for the HL-LHC do not show significant improvement in the moderate $\tan\beta$ region while HE-LHC can test a charged Higgs with mass up to 800 GeV for $\tan\beta \sim 20$ [59]. At low $\tan\beta$, the charged Higgs branching fractions for $H^{\pm} \to \tau\nu$ becomes strongly suppressed once the decay mode $H^{\pm} \to tb$ opens up, which is being taken seriously recently [58, 60]. With this decay channel, the ATLAS experiment has already ruled out charged Higgs with $m_{H^{\pm}} \sim 600$–900 GeV for $\tan\beta \sim 1$–0.5, and $m_{H^{\pm}} \sim 550$ GeV for $\tan\beta \sim 60$ [41].

In summary, the conventional decay channels are useful for studying 2HDMs. However, if the BSM Higgs mass spectrum is hierarchical, the branching fractions of the conventional decay channels are reduced by the opening up of the exotic decay channels. This in turn reduces the reach of the conventional channels and relaxes the current experimental direct search limits based on them. As a result, the exotic channels become complementary to the conventional search channels — when combined, they can cover most of the viable 2HDM parameter space at current and future hadron colliders.

3 The neutral Higgs channel: $A \to HZ$

3.1 Signal processes

As discussed in section 2.3, the requirements of unitarity and vacuum stability constrain the CP-odd state A to be heavier than the CP-even state, thereby opening up the exotic decay mode $A \to HZ$. A further leptonic decay of the Z-boson leads to a experimental signature that is both clean and covered by the conventional trigger menu of the LHC experiments. This makes the decay $A \to HZ$ the most promising exotic decay channel.

Below the top threshold, H will predominantly decay to either a pair of b-quarks or a pair of τ leptons. Although the branching fraction of the former ($\approx 90\%$) is significantly higher than that of the latter ($\approx 10\%$), it suffers from large SM backgrounds, making it experimentally challenging to detect. In contrast, the latter channel is much cleaner, making it particularly interesting at high luminosities at which sufficient statistics will be available to make up for its lower branching fraction.

If m_H is above the top threshold, that is, greater than twice the mass of the top quark, H will predominantly decay into top quark pairs except at large values of $t_\beta \gtrsim 30$, where the coupling of H to top quarks is suppressed. If m_H is relatively small, leptonic top decays will provide the most sensitive signal. On the other hand, if it is large, on the order of a TeV or greater, the top quarks in the final state can be highly boosted and top-tagging techniques can be profitably applied. The latter approach will work particularly well at a future 100 TeV pp collider, at which TeV-scale heavy Higgses will be produced in sufficient

JHEP06(2019)031

numbers. In this section we therefore consider the three dominant channels

$$pp \to A \to HZ \to (bb/\tau\tau/t_h t_h)\ell\ell \ . \tag{3.1}$$

While we focus on the $pp \to A \to HZ$ channel, we note that the same search can also be performed for the $pp \to H \to AZ$ channel.

3.2 Analysis

3.2.1 $bb\ell\ell$-channel

We first consider the $A \to HZ \to bb\ell\ell$ channel, which is the dominant decay channel for low mass scalars and has been subject to searches at both ATLAS [13] and CMS [14].

As discussed in [8], the dominant SM background to this channel is fully-leptonic top pair production ($tt \to bb\ell\ell + \not{E}_T$), followed by bottom-associated Z-boson production ($bbZ \to bb\ell\ell$) for $\ell = e, \mu$. Decays to τs are included in the tt background as well. Additional backgrounds from multi-boson production or mis-tagged jets play a sub-dominant role. The fully-leptonic top pair production background process is simulated with up to one additional jet and its cross-section normalized to 102 pb and 3714 pb at 14 TeV [61] and 100 TeV [62], respectively. The sub-leading $bbZ \to bb\ell\ell$ background is simulated at leading order taking into account a next-to-leading order (NLO) K-factor of 1.45 [63]. For a transverse momentum threshold of $p_b > 15$ GeV, this implies a background rate of 9.7 pb and 350 pb at 14 TeV and 100 TeV, respectively.

Both the signal and the background process are simulated using MadGraph 5 [64], interfaced with Pythia [65, 66] and Delphes 3 [67] for detector simulation. Each signal benchmark is simulated with the correct width and branching fractions as obtained from 2hdmc [68]. We then select events with at least two same-flavor leptons passing the trigger requirements $p_{T,\ell_1} > 20$ GeV and $p_{T,\ell_2} > 10$ GeV and two b-tagged jets with $p_{T,b} > 25$ GeV.[4] For these events, we construct a set of observables which is then used to train and test a boosted decision tree classifier. For the $bb\ell\ell$ channel, the set of observables includes:

- the transverse momenta of the leading b-tagged jet (p_{T,b_1}), the sub-leading b-tagged jet (p_{T,b_2}), the leading lepton (p_{T,ℓ_1}) and the sub-leading lepton (p_{T,ℓ_2})
- the invariant mass of the leptons ($m_{\ell\ell}$), the jets (m_{bb}) and the lepton-jet system ($m_{bb\ell\ell}$)
- the scalar sum of all the transverse energy (H_T) and the missing transverse energy ($\not{E}_T$).

Finally, a hypothesis test is performed for each benchmark point to obtain the projected statistical significance of the BSM hypothesis versus the SM. We assume a 10% systematic error in the background cross section.[5] More details of our analysis can be found in appendix A.

[4] Stronger selections cuts are applied at a 100 TeV collider for all the search channels (see appendix A).

[5] The typical systematic error at the LHC is between 20% and 50% [13]. However, the largest contributions arise from simulation statistics and background modeling which could be improved greatly at the future colliders, while theory uncertainties are below 10%. We adopted a value of 10% for the systematic uncertainty to take into account the theory uncertainties.

JHEP06(2019)031

3.2.2 $\tau\tau\ell\ell$-channel

With increasing luminosities, the reach of the $A \to HZ \to bb\ell\ell$ channel will be limited by systematic uncertainties in estimating the background rates. Such limitations do not apply to the $A \to HZ \to \tau\tau\ell\ell$ channel due to its clean final state with significantly smaller background rates. Thus, despite having a cross section roughly ten times lower than that of the $bb\ell\ell$ channel, the sub-leading $\tau\tau\ell\ell$ channel is expected to have a superior reach. This channel has been considered by CMS [14] and has already been found to provide a reach comparable to the $bb\ell\ell$ channel with the 8 TeV data set. In this work we focus on the case in which both τs decay hadronically, since this allows for a more precise reconstruction of the Higgs mass than the case in which one or both τs decay leptonically, with missing energy arising from neutrinos in the final state. Note that the reach can be further enhanced by combining the hadronic and leptonic decays, which is beyond the scope of this work.

The main SM background to the $A \to HZ \to \tau\tau\ell\ell$ signal comes from boson pair production with the subsequent decay into leptons, $(Z/h/\gamma^*)Z \to \tau\tau\ell\ell$. The corresponding cross sections at NLO for the $\tau\tau\ell\ell$ final state are 6.8 fb at 14 TeV [69] and 67 fb at 100 TeV [62] for invariant masses $m_{\tau\tau} > 100\,\text{GeV}$. Note that this includes both resonant production via ZZ and hZ dominating at small masses $m_{\tau\tau}$ as well as off-shell contributions dominating at large $m_{\tau\tau}$. Sub-dominant backgrounds, for example from ZWW production, were found to be negligible.

For this analysis, we select events with two same-flavor leptons with $p_{T,\ell_1} > 20\,\text{GeV}$ and $p_{T,\ell_2} > 10\,\text{GeV}$ and two τ-tagged jets with $p_{T,\tau} > 25\,\text{GeV}$ and consider the following list of observables:

- the transverse momenta of leading τ-tagged jet (p_{T,τ_1}), the sub-leading τ-tagged jet (p_{T,τ_2}), the leading lepton (p_{T,ℓ_1}) and the sub leading lepton (p_{T,ℓ_2})
- the invariant mass of the leptons ($m_{\ell\ell}$), the jets ($m_{\tau\tau}$) and the lepton-jet system ($m_{\tau\tau\ell\ell}$)
- the scalar sum of all the transverse energy (H_T) and the missing transverse energy ($\not{E}_T$).

3.2.3 $tt\ell\ell$-channel

With increasing collision energy, the daughter particle CP-even scalar H with mass above the top threshold can be produced efficiently. In this case, the reaches of both the $A \to HZ \to bb\ell\ell$ and the $A \to HZ \to \tau\tau\ell\ell$ channel are limited by statistics due to the suppressed branching fractions, especially in the small t_β region, while the $A \to HZ \to tt\ell\ell$ channel is expected to improve the reach for H above the top quark threshold. The decay products of H can have fairly large p_T for TeV-scale Higgses, leading to collimated top decay products. Therefore, the standard top reconstruction method for the leptonic decay mode will lose its efficiency. However, top-tagging techniques [70] developed in recent years could retain up to 30% of hadronic tops while rejecting most of the QCD events (see appendix B). For simplicity, in this work we focus on the case in which both tops decay hadronically, which allows for a more precise reconstruction of the Higgs mass. Note that mixed hadronic and

JHEP06(2019)031

leptonic top decays lead to another potentially interesting channel, $A \to HZ \to t_h t_\ell \ell\ell$, which is beyond the scope of this work.

The dominant SM background to this channel is the process $ttZ \to tt\ell\ell$. The corresponding cross section at NLO is 1.91 pb at 100 TeV [62]. We select events with two same-flavor leptons passing the trigger requirements $p_{T,\ell_1} > 20\,\text{GeV}$ and $p_{T,\ell_2} > 10\,\text{GeV}$ and two top-tagged jets with $p_{T,t} > 200\,\text{GeV}$. The following list of observables is used to train and test a BDT classifier:

- the transverse momenta of the leading top-tagged jet (p_{T,t_1}), the sub-leading top-tagged jet (p_{T,t_2}), the leading lepton (p_{T,ℓ_1}) and the sub-leading lepton (p_{T,ℓ_2})
- the invariant mass of the leptons ($m_{\ell\ell}$), the jets (m_{tt}) and the lepton-jet system ($m_{tt\ell\ell}$)
- the scalar sum of all the transverse energy (H_T) and the missing transverse energy ($\not{E}_T$).

3.3 Reach

As discussed in section 2.5, the production of A occurs primarily via gluon fusion in the small $\tan\beta$ region and bottom quark fusion in the large $\tan\beta$ region. We perform a separate analysis for each of these production modes and combine their significances when presenting the reach.

In figure 4, we present the discovery (dashed lines) and exclusion (solid lines) reach in the m_A vs. $\tan\beta$ plane for **BP-A** with $m_A = m_{H^\pm} > m_H$ (left panels) and **BP-B** $m_A > m_{H^\pm} = m_H$ (right panels) at the LHC, HL-LHC and a 100 TeV hadron collider for a fixed mass splitting between the heavy neutral Higgses of $\Delta m = m_A - m_H = 200\,\text{GeV}$. The top panels show the reach for the $bb\ell\ell$ and $t_h t_h \ell\ell$ final states while the bottom panels show the reach for the $\tau_h \tau_h \ell\ell$ final state.

At low values of $\tan\beta$, both the $H \to bb$ and $H \to \tau\tau$ channels are particularly sensitive at masses below the top threshold, $m_A = 2m_t + \Delta m \approx 550\,\text{GeV}$, while the branching fractions for these decays are strongly suppressed at larger masses due to the opening up of the $H \to tt$ channel. Increasing the luminosity to $3\,\text{ab}^{-1}$ at HL-LHC or a 100 TeV collider does not enhance the reach significantly. At large values of $\tan\beta$, the decay $H \to tt$ is strongly suppressed and so the $H \to bb$ and $H \to \tau\tau$ channels retain sensitivity for large masses.

The $bb\ell\ell$ channel is limited by systematic uncertainties and hence the reach does not increase much with increasing luminosities or center-of-mass energies. In contrast, the $\tau\tau\ell\ell$ channel has a much cleaner signature and therefore is mainly limited by statistical uncertainty and hence superior in sensitivity to the $bb\ell\ell$ channel. At $\tan\beta = 50$ the exclusion reach of the $\tau\tau\ell\ell$ channel extends up to ~ 1 TeV at the LHC, ~ 1.5 TeV at the HL-LHC and ~ 3 TeV at a 100 TeV pp collider. The maximal discovery regions are around 0.5 TeV, 1 TeV and 2.5 TeV for LHC, HL-LHC and 100 TeV pp collider, respectively.

The $H \to t_h t_h$ channel is able to probe scenarios with larger Higgs masses in the range $700\,\text{GeV} \lesssim m_A \lesssim 2\,\text{TeV}$ for small values of $\tan\beta \lesssim 3$. For smaller masses, the sensitivity of this search is limited by the efficiency of the hadronic top-tagging due to smaller typical

JHEP06(2019)031

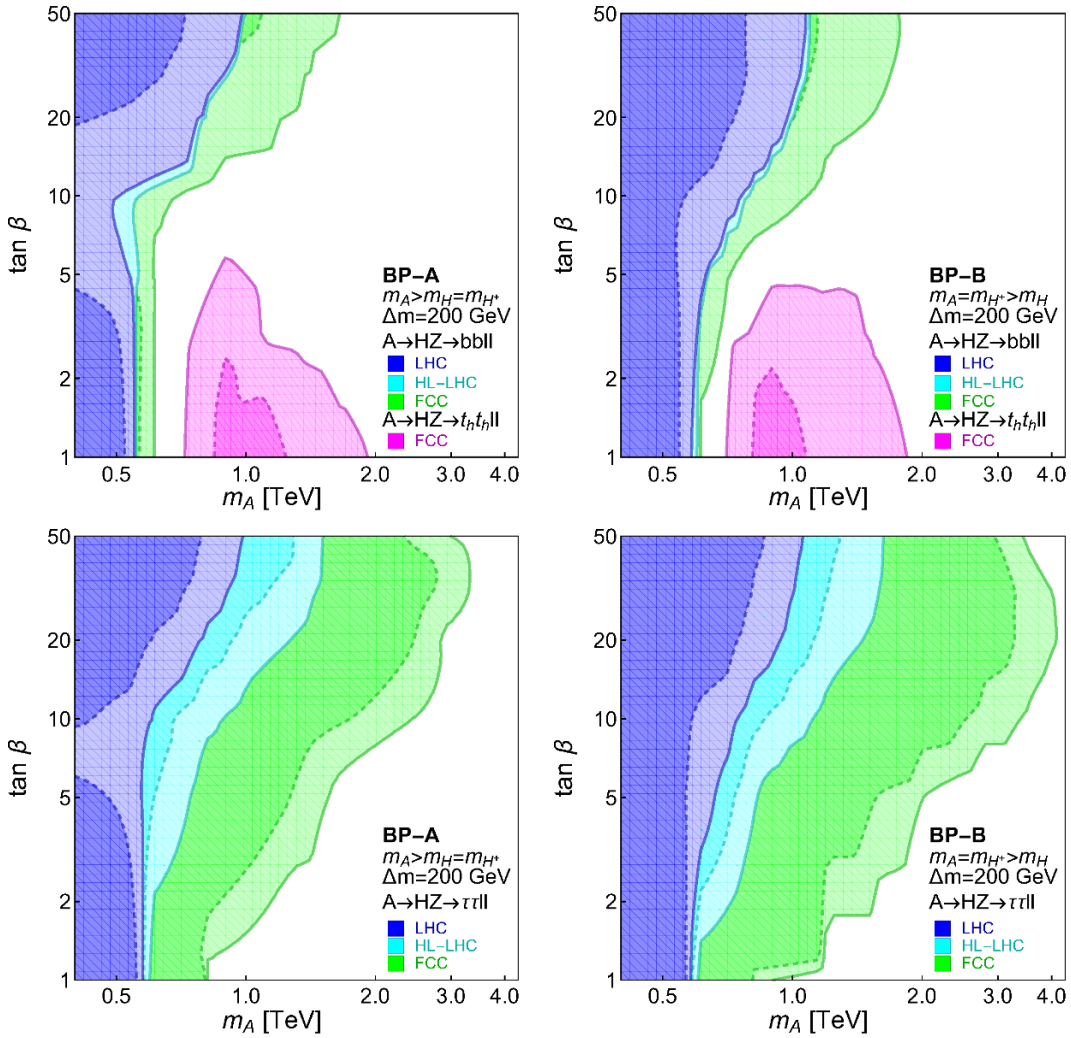

Figure 4. Discovery (dashed) and exclusion (solid) reach for **BP-A** (left) and **BP-B** (right) at the LHC (blue), HL-LHC (cyan) and a 100 TeV pp collider (green and magenta) in the $\tan\beta$ vs. m_A plane for $m_A - m_H = 200\,\text{GeV}$. We show the reach for the $bb\ell\ell$ and $t_ht_h\ell\ell$ channels (top), and $\tau\tau\ell\ell$ channel (bottom).

transverse momenta. In comparison, the conventional search channel, $ttH/A \to tttt$ [57], is more sensitive to heavy Higgs mass regions at small $\tan\beta$ due to its larger production cross sections, smaller dominant irreducible SM backgrounds, and certain discriminative kinematic features of $ttH/A \to tttt$ signal. At larger values of $\tan\beta$, this search loses sensitivity due to both the smaller Higgs production rates and the smaller Higgs branching fraction into top pairs.

While the heavy pseudoscalar A can decay either into HZ or $H^\pm W^\mp$ in **BP-A**, only the $A \to HZ$ channel is available in **BP-B**. Thus, the discovery and exclusion reach attainable in **BP-B** is greater than in **BP-A**.

JHEP06(2019)031

4 The charged Higgs channel: $A \to H^\pm W^\mp$

4.1 Signal processes

If the mass splitting between the pseudoscalar and charged Higgs is large enough ($m_A > m_{H^\pm} + m_W$), the additional decay channel $A \to H^\pm W^\mp$ opens up. This happens in scenarios such as **BP-A**, where $m_H = m_{H^\pm} < m_A$. In this case the branching fraction for the exotic decay mode $A \to H^\pm W^\mp$ is typically twice as large as that of the $A \to HZ$ decay mode which can be understood from the Goldstone equivalence theorem. The leptonic decay of the W-boson provides a clean experimental signature and permits the use of a lepton trigger, which makes the decay mode $A \to H^\pm W^\mp$ a promising exotic decay channel to explore.

If the charged Higgs is light ($m_{H^\pm} \lesssim m_t$), it will dominantly decay into either $\tau\nu$ at high t_β or cs at low values of t_β. However, such a light charged Higgs boson is excluded by the non-observation of the top decay $t \to H^+ b$ [42]. If the charged Higgs is heavier ($m_{H^\pm} > m_t$), the $H^\pm \to tb$ decay mode opens up and becomes dominant over the entire phase space. In this case the exotic decay channel $A \to H^\pm W \to tbW$ will have the same event topology as top-quark pair production, making background suppression the main challenge for this channel.

If the charged Higgs mass is relatively small ($m_{H^\pm} \sim$ a few 100 GeV), the top quark decay products will be both soft as well as spread out over the detector area. In this case leptonic top decays are expected to provide the most sensitive channel. However, at larger masses ($m_{H^\pm} \gtrsim 1$ TeV), the top quark from a heavy charged Higgs decay will be boosted and top-tagging techniques can be used to identify the top quark candidate. In contrast to leptonic top decays, which suffer from additional missing energy due to the neutrino in the final state, hadronic top decays also allow for a more precise reconstruction of the masses of the top quark and the charged Higgs. In this study, we therefore focus on the following production and decay chain:

$$pp \to A \to H^\pm W^\mp \to t_h b\, \ell\nu. \tag{4.1}$$

4.2 Analysis

After requiring a hadronic top-tagged jet in the final state, the leading irreducible background is semi-leptonic top pair production, $tt \to t_h b\ell\nu$, where $\ell = e, \mu, \tau$. The corresponding cross section at a 100 TeV collider is 15.1 nb at NNLO [62], which is reduced by a factor of roughly 0.2 once we require $p_{T,t} > 250$ GeV. Additional backgrounds arising from the production of a leptonically decaying W-boson in association with a boosted jet with $p_{T,j} > 250$ GeV, which could be misidentified as a top quark, were found to be small, $\sigma(W^\pm + j \to \ell^\pm\nu + j) = 0.43$ nb [62] and are further reduced upon including the mis-tagging rate for QCD jets $\epsilon_j \sim 10^{-3}$ (see appendix B). Similarly, backgrounds from single top production were found to be negligible.

We select events containing one lepton with $p_{T,\ell_1} > 20$ GeV, at least one top-tagged jet with $p_{T,t_1} > 200$ GeV, at least one b-tagged jet with $p_{T,b} > 50$ GeV and a small amount of missing transverse energy, $\not{E}_T > 20$ GeV. The following set of observables is then used to train and test a BDT classifier:

JHEP06(2019)031

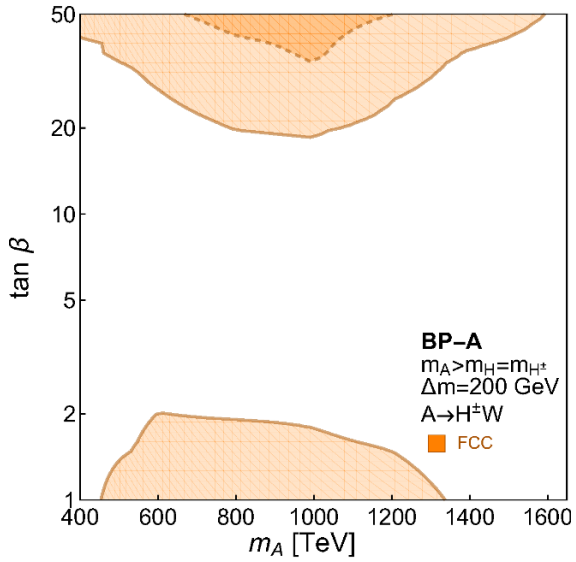

Figure 5. Reach for the exotic decay channel $A \to H^{\pm}W^{\mp} \to t_h b l \nu$ for **BP-A** at a 100 TeV pp collider in the $\tan\beta$ vs. m_A plane for $m_A - m_{H^{\pm}} = 200\,\text{GeV}$. The solid and dashed line correspond to the exclusion and discovery reach, respectively.

- the transverse momenta of the leading top-tagged jet (p_{T,t_1}), the leading b-tagged jet (p_{T,b_1}) and the leading lepton (p_{T,ℓ_1}).
- the invariant masses of the jets (m_{tb}) and the lepton-jet system ($m_{tb\ell\nu}$), and the angular separation of the jets (ΔR_{tb}).
- the scalar sum of the transverse energy (H_T) and the missing transverse energy ($\not{E}_T$).

To reconstruct the mass of the heavy neutral Higgs ($m_{tb\ell\nu}$), we reconstruct the neutrino momentum from $\not{E}_T$ following the method shown in ref. [71].

4.3 Reach

In figure 5 we present the reach for the exotic decay channel $A \to H^{\pm}W^{\pm}$ for **BP-A**. Note that this channel is not open in **BP-B**, where $m_{H^{\pm}} = m_A$. We find that the LHC is insensitive to this channel due to a low heavy Higgs production rate and insufficiently boosted decay products. In contrast, a 100 TeV collider will be able to produce a sufficient number of heavy Higgses with $\sim$ TeV scale masses that can decay into top quarks with the sizable boosts necessary for the use of top-tagging techniques. The corresponding exclusion and discovery reaches are shown as solid and dashed lines, respectively.

At small values of t_β (< 2) where the pseudoscalar A is dominantly produced via gluon fusion, the exclusion reach can be up to $m_A \simeq 1.3\,\text{TeV}$. At large t_β ($\gtrsim 20$) the bottom-quark associated production process dominates and this channel can discover a CP-odd scalar A with mass up to 1.2 TeV or exclude CP-odd scalars with masses up to 1.6 TeV. The low reach in the wedge region ($2 \lesssim t_\beta \lesssim 20$), results from the small production cross section for both the gluon fusion and the bottom quark fusion production of the CP-odd scalar A.

JHEP06(2019)031

Finally, we note that the reach of this channel is dominated by systematic uncertainties, given the large top pair backgrounds. In particular, when estimating the reach we assumed a 10 % systematic uncertainty on the background rate. A better theoretical understanding of QCD processes, especially top-pair production, will be extremely important for accurate background estimation at future 100 TeV colliders to reduce the systematic uncertainties.

5 Exotic charged Higgs decays: $H^\pm \to HW^\pm$

5.1 Signal processes

While in the previous section we considered exotic decays of neutral Higgses to charged Higgses, it is also possible for charged Higgses themselves to undergo exotic decays. As discussed in section 2.4, the only viable exotic decay mode for heavy charged Higgses in hierarchical 2HDMs in the alignment limit is the decay $H^\pm \to HW^\pm$, which appears in **BP-B** when the mass splitting between the charged and neutral Higgses is sufficiently large ($m_{H^\pm} > m_H + m_W$). As discussed in section 2.5, the charged Higgs is mainly produced in association with a top and bottom quark ($pp \to H^\pm tb$), which leads to a busy final state topology ($H^\pm tb \to HW^+W^-bb$).

If the daughter Higgs H is light ($m_H < 2m_t$), it will dominantly decay into pairs of b-quarks and τ leptons with branching fractions of $\sim 90\%$ and $\sim 10\%$ respectively. Despite its larger branching fraction, the $H \to bb$ decay channel remains experimentally challenging, due to the large hadronic SM backgrounds associated with it.[6] In contrast, the $H \to \tau\tau$ decay channel can lead to a same-sign di-lepton signature where one lepton arises from a leptonic τ-decay and the other from a leptonic W-decay. As shown in [10], this signature allows for the effective suppression of SM backgrounds — in particular, the background from top pair production.

If the daughter Higgs is heavier ($m_H > 2m_t$), it will dominantly decay into pairs of top quarks, leading to a final state equivalent to four top quarks. Searches for this channel therefore will be extremely challenging due to the large hadronic SM backgrounds. However, the authors of [73] have proposed to utilize the possible tri-lepton and same-sign di-lepton signatures and have shown that these can be promising for larger values of m_H. In this study we consider the following signal production and decay chain:

$$gg \to H^\pm tb \to H\ W^+W^-\ bb \to \tau\tau\ W^+W^-\ bb. \tag{5.1}$$

with a focus on the same-sign di-lepton final state.

5.2 Analysis

As mentioned above, we consider the case in which one of the W bosons and one of the τ leptons decay hadronically, and the other W boson and τ lepton decay leptonically. The resulting final state permits the same-sign di-lepton signature $\ell^\pm\ell^\pm + 2b + 2j + \tau_h + \not{E}_T$, which allows the suppression of most SM backgrounds.

[6] The authors of [72] have shown that a jet substructure analysis of the pseudoscalar and W jets can be used to significantly reduce hadronic backgrounds and provide some reach for low values of m_H and $\tan\beta$.

JHEP06(2019)031

The remaining background is dominated by the $tt\tau\tau$ production process, where at least one of the top quarks decays leptonically (where the definition of leptons includes τs) [10]. The τs originate from the decay of a neutral SM boson (Z, h, γ^*). As discussed below, the neutral Higgs candidate H is reconstructed by combining the momentum of the hadronic τ with the momentum of the softer lepton. A large invariant mass of the Higgs candidate in $tt\tau\tau$ background events typically only arises when combining a hadronic τ from boson decay with a lepton from top quark decay, providing a smooth background spectrum. Using MadGraph 5, we obtain a cross section for $t_{h/\ell}t_\ell\tau\tau$ production of 886 fb for a 100 TeV collider, with the largest individual contribution corresponding to the resonant backgrounds ttZ and tth. For completeness, we also consider the sub-dominant backgrounds, which can provide a same-sign di-lepton signature, $ttW \to t_\tau t_\ell \ell\nu$ and $ttZ \to t_\tau t_\ell \ell\ell$ with cross sections of 99 fb and 166 fb, respectively.

Following the analysis strategy outlined in [10], we select events with two same-sign leptons, one or two b-tagged jets, one τ-tagged jet with sign opposite that of the leptons, and at least two untagged jets. We loop over all combinations of the untagged jets and choose the combination that has invariant mass closest to the mass of the W boson. We reconstruct the leptonically-decaying W boson by first reconstructing the neutrino momentum using the procedure in [71] and then combining it with the momentum of the hardest lepton. We then combine the momentum of the τ-tagged jet with the momentum of the softer lepton to approximate the momentum of the neutral Higgs boson H. Finally, we combine the H candidate with the W candidate that gives the mass closest to the mass of the charged Higgs. The input features for the BDT classifier are the following:

- the transverse momenta of the leading lepton (p_{T,ℓ_1}), the leading untagged jet (p_{T,j_1}), the b-tagged jet ($p_{T,b}$), and the τ-tagged jet (p_{T,τ_h}).
- the invariant masses of the neutral and charged Higgs candidates ($m_{\tau_h\ell_2}$ and $m_{\tau_h\ell_2 W}$).
- the missing transverse energy ($\not{E}_T$).

5.3 Reach

In figure 6, we show the discovery and exclusion reaches (the dashed and solid lines respectively) for the exotic decay channel $H^\pm \to HW$ for **BP-B**. The reach at the 14 TeV LHC [10] for this channel is limited by the low production cross section of heavy charged Higgs bosons, and thus we only show the reach for a 100 TeV pp collider, which will be able to produce charged Higgses with TeV-scale masses in large numbers.

Below the top-quark threshold, $m_A < 2m_t + \Delta m \approx 550$ GeV, the $H \to \tau\tau$ channel can probe the entire range of $\tan\beta$. Above this threshold, the $H \to tt$ decay channel opens up, eliminating the reach at lower values of $\tan\beta$. In the interesting wedge region, around $t_\beta = 10$, this channel can discover scenarios with charged Higgs masses up to 1.7 TeV and exclude charged Higgses with masses up to 2.5 TeV.

6 Reach in benchmark planes

In figure 7, we present the exclusion and discovery reaches in the $\Delta m = m_A - m_H$ versus m_A plane for **BP-A** (left panel) and **BP-B** (right panel) with $\tan\beta = 1.5$. As dis-

JHEP06(2019)031

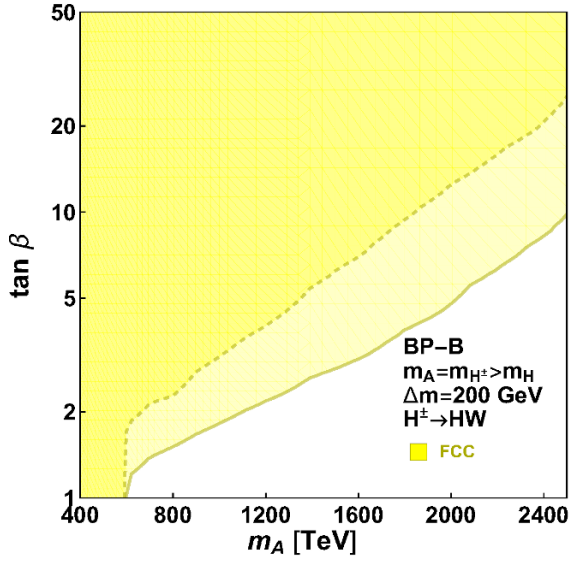

Figure 6. Reach for the exotic decay channel $H^{\pm} \to HW \to \tau\tau\, bb\, WW$ for **BP-B** at a 100 TeV pp collider in the $\tan\beta$ vs. m_A plane for $m_A - m_H = 200\,\text{GeV}$. The solid and dashed line correspond to the exclusion and discovery reach, respectively.

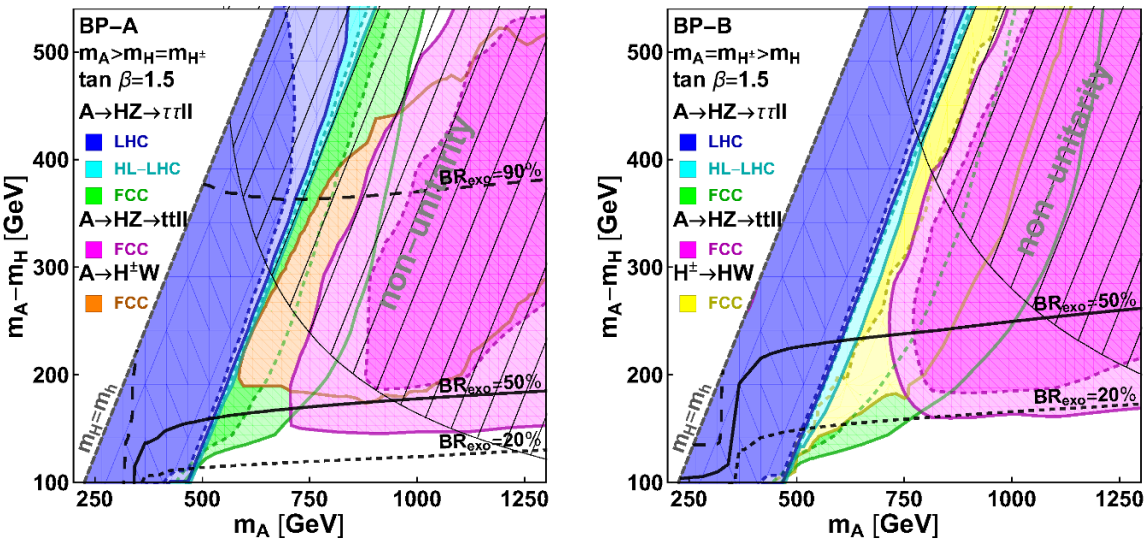

Figure 7. Reach for the exotic Higgs decay channels at the LHC, HL-LHC and 100 pp TeV collider for **BP-A** (left) with the mass hierarchy $m_H = m_{H^{\pm}} < m_A$ and **BP-B** (right) with the mass hierarchy $m_H < m_{H^{\pm}} = m_A$. The results are presented in the m_A vs. $m_A - m_H$ plane for a fixed value of $t_\beta = 1.5$. We show the projected sensitivity of the $A \to \tau\tau\ell\ell$ channel (blue/cyan/green) as discussed in section 3.2.2, the $A \to tt\ell\ell$ channel (magenta) as discussed in section 3.2.3, the $A \to H^{\pm}W^{\mp}$ (orange) as discussed in section 4.2 and the $H^{\pm} \to HW^{\pm}$ channel (yellow) as discussed in section 5.2. The exclusion and discovery reaches for each channel are shown as solid and dashed lines respectively. The hatched regions are excluded by unitarity constraints and the thick black lines indicate the branching fraction for exotic Higgs decays of the heavy pseudoscalar A.

JHEP06(2019)031

cussed in section 2.4, these two benchmark scenarios, corresponding to the mass hierarchies $m_H = m_{H^\pm} < m_A$ and $m_H < m_{H^\pm} = m_A$ respectively, have been found to be representative of hierarchical 2HDMs. In particular, they are permitted by theoretical considerations of unitarity and vacuum stability as well as electroweak precision measurements. For the purpose of illustration, we consider $\tan\beta = 1.5$. This choice is representative of the interesting low $\tan\beta$ region, which will be particularly hard to constrain using the conventional searches such as $A/H \to \tau\tau$ and $H^\pm \to \tau\nu$ which are expected to provide the best sensitivity at higher values of $\tan\beta$.

For the $A \to HZ \to \tau\tau\ell\ell$ channel, the blue, cyan, and green regions show the reaches at the LHC, HL-LHC, and a future 100 TeV collider, respectively. For the $A \to HZ \to tt\ell\ell$ channel, as well as the channels involving charged Higgs bosons, $A \to H^\pm W$ and $H^\pm \to AW$, the reaches at a 100 TeV collider are shown in magenta, orange and yellow, respectively. For each of the six colors, we distinguish between discovery and exclusion regions using differing line styles and opacities for the contours and the shading of the regions they enclose. Regions that are more opaque and bounded by dashed contours correspond to discovery, and regions that are more transparent and bounded by solid contours correspond to exclusion (the discovery regions are always subsets of the exclusion regions).

The highest sensitivity at low values of m_H is provided by the $A \to HZ \to \tau\tau\ell\ell$ channel. At both the LHC (blue) and HL-LHC (cyan), the reach extends up to $m_H = 2m_t$, resulting in almost straight lines for the sensitivity contours. This can be understood from the fact that the $H \to tt$ channel quickly becomes dominant once it is kinematically accessible in the low t_β regions, with a branching fraction close to 100%. Therefore, in this channel, the HL-LHC will not be able to improve the expected reach for hierarchical 2HDMs compared to the LHC. In contrast, a future 100 TeV collider (green) will be able to provide a sufficient event rate for the $A \to HZ \to \tau\tau\ell\ell$ channel to significantly extend the reach towards higher masses $m_H > 2m_t$, despite the suppressed branching fraction for $H \to \tau\tau$. Comparing both benchmark planes, the reach for **BP-A** is slightly reduced compared to **BP-B** due to the suppressed branching fraction for the $A \to HZ$ in the presence of the additional decay channel $A \to H^\pm W$. The $A \to HZ \to bb\ell\ell$ channel is limited by systematic errors, resulting in a significantly weakened sensitivity, and is therefore not shown in figure 7. Scenarios with larger Higgs masses m_H can be probed with the decay channel $A \to HZ \to tt\ell\ell$. We focus on the case of hadronically decaying top quarks, which can be identified using top tagging techniques, and present the reach at a 100 TeV hadron collider (magenta). The sensitivity is weakened in regions with lower Higgs masses $m_H \lesssim 600\,\text{GeV}$ in which the top quarks will no longer have sufficient transverse momentum ($p_{T,t} \sim (m_H - 2m_t)/2$) to exceed the top tagging threshold ($p_{T,t} > 200\,\text{GeV}$). As before, the reach in **BP-A** is reduced relative to **BP-B** due to the lower branching fraction for the decay $A \to HZ$.

In addition to the neutral Higgs channel $A \to HZ$, hierarchical 2HDMs can also be probed via exotic Higgs decays involving charged Higgs bosons. **BP-A** permits the additional exotic Higgs decay channel $A \to H^\pm W$. Above the top threshold, the charged Higgs decays predominantly into $H^\pm \to tb$. Again we focus on subsequent hadronic top decays, which permit the use of top tagging techniques, and obtain the projected sensitivity

JHEP06(2019)031

at a 100 TeV collider (orange). For smaller charged Higgs masses ($m_{H^\pm} \lesssim 400\,\text{GeV}$), the sensitivity of this search channel is limited by the efficiency of the hadronic top-tagging due to smaller typical transverse momenta $p_{T,t} \sim (m_{H^\pm} - m_t)/2$. Note that the slightly larger typical $p_{T,t}$ in $H^\pm \to tb$ decays compared to $H \to tt$ decays results in a mildly extended reach towards lower masses compared to the $A \to HZ \to tt\ell\ell$ channel.

The exotic decay of a charged Higgs boson $H^\pm \to HW$ is permitted only in the mass hierarchy of **BP-B**. While searches for this channel at the LHC suffer from a low charged Higgs production rate, the production cross section increases significantly towards higher energies. We obtain the projected sensitivity at a 100 TeV hadron collider (yellow) considering the neutral Higgs decay $H \to \tau\tau$. Below the $H \to tt$ threshold, this channel provides 5-σ discovery at a future 100 TeV collider, which is comparable with $A \to HZ \to \tau\tau\ell\ell$ channel.

As discussed in section 2.4, unitarity disfavors large mass splittings $m_A - m_H$ at large Higgs masses m_A. This constraint is represented by the hatched region in figure 7. In particular, unitarity constrains a larger region of parameter space for **BP-A** than for **BP-B**, imposing upper bounds on the mass splittings of $5(m_A^2 - m_H^2) < 8\pi v^2$ and $3(m_A^2 - m_H^2) < 8\pi v^2$, respectively.

To indicate the importance of exotic Higgs decays relative to the conventional Higgs decays, we also show branching fraction for exotic Higgs decays of the heavy pseudoscalar A as black contours in figure 7. The dotted, solid, and dashed black contours correspond to branching fractions of 20%, 50%, and 90%, respectively. We can see that a future 100 TeV hadron collider will be able to probe most regions of the Type-II 2HDM parameter space that survive current theoretical and experimental constraints with sizable exotic branching fractions using the combination of all the viable heavy Higgs exotic decay channels.

7 Conclusion

While most direct searches for an BSM Higgs sector focus on the conventional decays of the corresponding Higgs bosons, additional exotic decays of these states can arise if the BSM Higgs sector is hierarchical. These exotic decays include the decay of a heavy Higgs to two lighter Higgses, or to a lighter Higgs and a SM gauge boson. The presence of those exotic decay channels weaken the bounds of conventional searches, but also open up new complementary search channels.

In this paper, we studied the sensitivity of the LHC, HL-LHC and s 100 TeV pp collider to exotic Higgs decays in Type-II 2HDMs. As discussed in section 2, theoretical considerations such as unitarity and vacuum stability and experimental limits, e.g. from electroweak precision measurements, severely constrain the parameter space of hierarchical 2HDMs. Besides the fully degenerate case $m_H \approx m_A \approx m_{H^\pm}$, there are two benchmark planes that are viable under the alignment limit: **BP-A** ($m_A > m_H = m_{H^\pm}$) with $A \to HZ/H^\pm W^\mp$ and **BP-B** ($m_A = m_{H^\pm} > m_H$) with $A \to HZ$, $H^\pm \to HW^\pm$.

A 100 TeV pp collider provides the opportunity to probe exotic decays of heavy Higgses with top quarks in the final state. Top quarks originating from the decay of a heavy Higgs are typically boosted, permitting the use of top tagging techniques to identify them. This

JHEP06(2019)031

allows us to take advantage of the large decay rates of heavy Higgses into top quarks while also getting a handle on QCD backgrounds.

To obtain the projected reach of the considered exotic Higgs decay channels, we perform a multivariate analysis using boosted decision tree classifiers which are trained to distinguish between the signal events and the SM background events. We find that the best sensitivity is provided by the exotic decay channel $A \to HZ$ due to its clean final state. Regions of parameter space with low values of m_H ($m_H < 2m_t$) and large values of $\tan\beta$ can efficiently be probed with the final states $bb\ell\ell$ and $\tau\tau\ell\ell$, where the $\tau\tau\ell\ell$ channel has a better reach compared to $bb\ell\ell$ channel due to the significantly lower backgrounds. For moderate mass splittings ($m_A - m_H = 200\,\text{GeV}$) and large values of $\tan\beta$ (> 10), a 100 TeV pp collider can discover (at 5σ) and exclude (at 95% C.L.) Higgs masses up to $m_A \approx 3\,\text{TeV}$ and 4 TeV, respectively. In the low $\tan\beta$ region above the top-pair threshold, the $tt\ell\ell$ channel is complementary to $\tau\tau\ell\ell$, extending the reach to about $m_A \approx 1.2\,\text{TeV}$ (2 TeV) for discovery (exclusion).

Hierarchical 2HDMs can further be probed via exotic decay channels involving the charged Higgs boson. In the mass hierarchy corresponding to **BP-A**, the exotic decay channel $A \to H^\pm W$ is kinematically open. Using the dominant charged Higgs decay mode $H^\pm \to tb$, a 100 TeV collider can exclude Higgs masses up to $m_A \approx 1.6\,\text{TeV}$ at large $\tan\beta$ (≈ 50) and about $m_A \approx 1.3\,\text{TeV}$ at small $\tan\beta$ (≈ 1) for a mass splitting of $m_A - m_H = 200\,\text{GeV}$. In **BP-B**, exotic decays of the charged Higgs $H^\pm \to HW$ become kinematically permissible. We analyze this decay considering $tbH^\pm$ associated charged Higgs production and the subsequent decay of the neutral Higgs $H \to \tau\tau$, which permits for a same-sign di-lepton signature. For moderate mass splittings ($m_A - m_H = 200\,\text{GeV}$) and values of $\tan\beta$ (≈ 10), a 100 TeV pp collider can discover (exclude) Higgs masses up to $m_{H^\pm} \approx 1.7\,\text{TeV}$ and 2.4 TeV, respectively. The channel $H \to tt$ could provide additional reach at low values of $\tan\beta$ above the top pair threshold [73].

Combining all the aforementioned exotic decay channels, we present the reach in the benchmark planes **BP-A** and **BP-B** for $\tan\beta = 1.5$ in figure 7. All three channels complement each other nicely: final states with τs prove to be the most sensitive channels for regions with relatively low values of m_A, and, as might be expected, final states with tops are useful above the top threshold. We find that these exotic decay channels can probe most of the parameter space in which their branching fraction is sizable, and are thus complementary to the conventional decay channels for heavy non-SM Higgses. Additionally, if a future 100 TeV collider observes the $A \to HZ$ channel, it would imply the existence of additional exotic decay channels involving the charged Higgs, which will be observable in many parts of the parameter space.

While most of the recent searches for additional Higgs bosons have focused on conventional decay channels, searches using exotic decay channels have just started [13, 14]. At a possible high energy future hadron collider, both the exclusion and the discovery reach for non-SM Higgses will be greatly enhanced compared to that of the LHC. The discovery of a non-SM heavy Higgs would serve as unambiguous evidence for new physics beyond the SM and could also provide valuable insights into mechanism underlying electroweak symmetry breaking.

JHEP06(2019)031

Acknowledgments

We would like to thank Ahmed Ismail for providing the production cross section of the charged Higgs at a 100 TeV pp collider. An allocation of computer time from the UA Research Computing High Performance Computing (HPC) and High Throughput Computing (HTC) at the University of Arizona is gratefully acknowledged. FK is supported by the U.S. National Science Foundation under the grant PHY-1620638. AP, HS, and SS were supported by the Department of Energy under Grant DE-FG02-13ER41976/DE-SC0009913. HL was supported by the National Natural Science Foundation of China (NNSFC) under grant No. 11635009 and Natural Science Foundation of Shandong Province under grant No. ZR2017JL006.

A Collider analysis methodology

In this section, we describe the details of the methodology we employ for our collider analysis: for each set of considered model parameters, we generate Monte Carlo event samples for both signal and background processes, train a BDT classifier to distinguish between signal and background events and perform a hypothesis test to obtain the expected statistical significance.[7]

The production cross sections for the heavy pseudoscalar A are calculated using SusHi [45–47] at NNLO. The charged Higgs productions rates have been adopted from [48] and therein were calculated[8] using Prospino [49, 50]. The decay width and branching fraction for each simulated signal benchmark point is calculated using the 2hdmc package [68].

We simulate parton-level events using MadGraph 5 and MadEvent [64, 74] with a modified 2HDM model, 2HDM-HEFT [75], created using FeynRules. This is followed by showering and hadronization using Pythia [65, 66], and fast detector simulation using Delphes 3 [67]. For the 14 TeV LHC and HL-LHC scenarios, we used the default Delphes detector cards in MadGraph. For the 100 TeV scenario, we used the Delphes detector card devised by the FCC-hh working group [76]. In particular, we adopt the following basic selection cuts for detector reconstruction from the Delphes cards listed above:

$$\begin{aligned}
\textbf{LHC/HL-LHC:}\quad & p_{T,\ell} > 10\,\text{GeV}, \quad p_{T,j/b/\tau} > 20\,\text{GeV}, \quad \Delta R > 0.5, \\
& |\eta_\ell| < 2.5, \qquad |\eta_j| < 5.0, \qquad |\eta_{b/\tau}| < 2.5 \\
\textbf{100 TeV:}\quad & p_{T,\ell} > 20\,\text{GeV}, \quad p_{T,j/b/\tau} > 50\,\text{GeV}, \quad \Delta R > 0.3, \\
& |\eta_\ell| < 6.0, \qquad |\eta_j| < 6.0, \qquad |\eta_{b/\tau}| < 6.0
\end{aligned} \tag{A.1}$$

where ΔR is the angular distance between any two objects.

The reconstructed-level events from Delphes are filtered through a series of trigger and identification cuts (described in sections 3.2, 4.2, and 5.2), after which a set of features were collected for each simulated collision event to serve as inputs to gradient boosted decision tree (BDT) classifiers [77] implemented in TMVA [78]. The set of input features

[7] The source code for the analysis in section 5 is available at https://github.com/adarshp/ExoticHiggs.
[8] We thank Ahmed Ismael for providing us with the production cross sections for the charged Higgs.

JHEP06(2019)031

included both low-level features such as the transverse momenta of individual particles, and physically-motivated high-level features such as the invariant masses of combinations of particle momenta. The events were then divided into training and test sets, and we trained our classifiers on the training sets with the following hyperparameters:

- The number of trees was set to 1000.
- The maximum depth of each tree was set to 3.
- Bagging was employed, with the bagged sample fraction set to 0.6.
- The Gini index was used as the separation criterion for node splitting.

The classifiers were then used to compute the BDT response value for signal and background events in the test set. We then scanned across a range of response values to determine the optimal cutoff with corresponding values of the total number of leftover signal (s) and background (b) events that resulted in the greatest discovery and exclusion significance. The values of s and b were obtained by multiplying their respective cross-sections by the integrated luminosity, which was taken to be $300\,\text{fb}^{-1}$ for the LHC, and $3000\,\text{fb}^{-1}$ for the HL-LHC and the 100 TeV collider.

Generating a large enough number of Monte Carlo events to estimate the backgrounds at a 100 TeV collider was a technically challenging task. For certain points in parameter space, a series of cuts could reduce the number of expected background events to zero. However, in such cases, we artificially set a minimum three background events, i.e. $b = 3$, to ensure that our significance estimates are not overly optimistic.

To estimate the median expected discovery and exclusion significances, Z_{disc} and Z_{excl}, we follow [79–81] and use the following expressions:

$$\begin{aligned} Z_{\text{disc}} &= \sqrt{2\left[(s+b)\ln\left(\frac{(s+b)(1+\epsilon^2 b)}{b+\epsilon^2 b(s+b)}\right)-\frac{1}{\epsilon^2}\ln\left(1+\epsilon^2\frac{s}{1+\epsilon^2 b}\right)\right]} \\ Z_{\text{excl}} &= \sqrt{2\left[s-b\ln\left(\frac{b+s+x}{2b}\right)-\frac{1}{\epsilon^2}\ln\left(\frac{b-s+x}{2b}\right)-(b+s-x)\left(1+\frac{1}{\epsilon^2 b}\right)\right]} \\ \text{with}\quad x &= \sqrt{(s+b)^2-4\epsilon^2 s b^2/(1+\epsilon^2 b)}. \end{aligned} \tag{A.2}$$

Here ϵ is the relative systematic uncertainty of the background rate. In the special case of vanishing systematic uncertainty $\epsilon \to 0$ these expressions simplify to

$$Z_{\text{disc}}^{\epsilon=0} = \sqrt{2[(s+b)\ln(1+s/b)-s]}, \qquad Z_{\text{excl}}^{\epsilon=0} = \sqrt{2[s-b\ln(1+s/b)]} \tag{A.3}$$

In the limit of a large number of background events, $b \gg s$, these expressions further simplify to the well known Gaussian approximations $Z_{\text{disc}} \approx s/\sqrt{b}$ and $Z_{\text{excl}} \approx s/\sqrt{s+b}$. In this work we choose a systematic uncertainty of $\epsilon = 10\%$ for both the LHC and the 100 TeV collider. We define regions with $Z_{\text{disc}} \geq 5$ as discoverable regions, and regions with $Z_{\text{excl}} \leq 1.645$ as regions that can be excluded at 95% CL.

JHEP06(2019)031

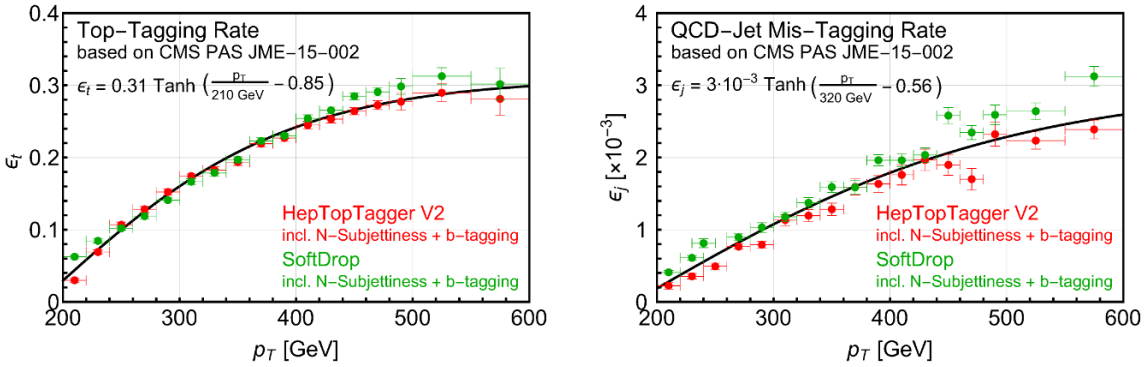

Figure 8. Top-tagging efficiencies (left) and QCD-jet mis-tagging rate (right) for the HEPTopTagger (red) and SoftDrop (green) as adapted from the CMS study [70]. The analytic parameterization used in this study is shown as a solid black line.

B Simulation of top-tagging

When an energetic top quark decays hadronically, its decay products are collimated and form a big jet, often called a *fat jet*. The size of a top-initiated fat jet is given by $R \sim 2m_t/p_{T,t}$, which implies that only boosted top quarks with $p_T > 250\,\mathrm{GeV}$ will be able to form a fat jet of size $R < 1.5$. While top-initiated fat jets show a characteristic substructure with subjets corresponding to the individual top decay products, such features are not present in QCD jets. Top-taggers are tools that analyze the fat jet's substructure to distinguish top-initiated from QCD initiated fat jets. Many ideas and techniques have been developed within the last year: QCD-based taggers like the HEPTopTagger [19–21] or the Johns Hopkins Tagger [22], Event-shape based tagger like N-subjettiness [23] or template-overlap method based taggers like the TemplateTagger [82]. A (not so recent) review about top tagging can be found in [83].

While most of the early taggers rely on only one analysis strategy, the more modern top taggers combine different approaches using machine learning tools. Examples include the HEPTopTagger Version-2 [84], the Deep-Top Tagger [24] (focusing on low p_T), and the Deep Neural Network Tagger [85] (same idea, focusing on high p_T). A recent summary comparing modern top tagging approaches has been published by CMS [70].

However, these techniques are usually computationally intensive, making them impractical for exploratory phenomenological studies such as this one. For this reason, we use a *parametric* approach, implementing a DELPHES top-tagging module inspired by the built-in b-tagging module. We first reconstruct all fat jets with the size of $R = 1.5$ using the Cambridge-Aachen algorithm [86] as implemented in FASTJET 3 [87]. We then assert that a fat jet is top quark initiated if a parton-level top quark is found within a cone with a radius $R = 0.8$ (we find that varying R between 0.8 and 1.5 will not affect the results). Leptonically-decaying top quarks are rejected by vetoing fat jets with leptons in the jet cone. Once a fat jet is determined to be top-initiated, we apply a top-tagging efficiency ϵ_t for each of these fat jets. For QCD initiated fat jets, a misidentification rate ϵ_j is applied.

In figure 8 we show the top-tagging rate (left) and QCD-jet mis-tagging rate (right) as adapted from figure 10 in the CMS study [70]. As representative examples we show the per-

JHEP06(2019)031

formance of the HEPTopTagger V2 [84] and SoftDrop [88] in combination with groomed N-subjettiness and b-tagging. Both taggers have similar tagging and mis-tagging rates which are roughly independent of number of pile-up vertices. We parameterize their performance using an analytic form for top-tagging efficiency ϵ_t and QCD-jet mis-identification rate ϵ_j and obtain

$$\epsilon_t = 0.31 \tanh(p_T/210\,\text{GeV} - 0.85) \quad \text{and} \quad \epsilon_j = 0.003 \tanh(p_T/320\,\text{GeV} - 0.56). \tag{B.1}$$

References

[1] ATLAS collaboration, *Observation of a new particle in the search for the Standard Model Higgs boson with the ATLAS detector at the LHC*, *Phys. Lett.* **B 716** (2012) 1 [arXiv:1207.7214] [INSPIRE].

[2] CMS collaboration, *Observation of a new boson at a mass of 125 GeV with the CMS experiment at the LHC*, *Phys. Lett.* **B 716** (2012) 30 [arXiv:1207.7235] [INSPIRE].

[3] G.C. Branco, P.M. Ferreira, L. Lavoura, M.N. Rebelo, M. Sher and J.P. Silva, *Theory and phenomenology of two-Higgs-doublet models*, *Phys. Rept.* **516** (2012) 1 [arXiv:1106.0034] [INSPIRE].

[4] J. Gu, H. Li, Z. Liu, S. Su and W. Su, *Learning from Higgs Physics at Future Higgs Factories*, *JHEP* **12** (2017) 153 [arXiv:1709.06103] [INSPIRE].

[5] N. Chen, T. Han, S. Su, W. Su and Y. Wu, *Type-II 2HDM under the Precision Measurements at the Z-pole and a Higgs Factory*, *JHEP* **03** (2019) 023 [arXiv:1808.02037] [INSPIRE].

[6] CEPC-SPPC Study Group, *CEPC-SPPC Preliminary Conceptual Design Report. 1. Physics and Detector*, http://cepc.ihep.ac.cn/preCDR/volume.html (2015).

[7] M. Benedikt and F. Zimmermann, *Future Circular Collider Study, Status and Progress*, https://indico.cern.ch/event/550509/contributions/2413230/attachments/1396002/2128079/170116-MBE-FCC-Study-Status_ap.pdf (2017).

[8] B. Coleppa, F. Kling and S. Su, *Exotic Decays Of A Heavy Neutral Higgs Through HZ/AZ Channel*, *JHEP* **09** (2014) 161 [arXiv:1404.1922] [INSPIRE].

[9] T. Li and S. Su, *Exotic Higgs Decay via Charged Higgs*, *JHEP* **11** (2015) 068 [arXiv:1504.04381] [INSPIRE].

[10] B. Coleppa, F. Kling and S. Su, *Charged Higgs search via $AW^{\pm}/HW^{\pm}$ channel*, *JHEP* **12** (2014) 148 [arXiv:1408.4119] [INSPIRE].

[11] F. Kling, A. Pyarelal and S. Su, *Light Charged Higgs Bosons to AW/HW via Top Decay*, *JHEP* **11** (2015) 051 [arXiv:1504.06624] [INSPIRE].

[12] F. Kling, J.M. No and S. Su, *Anatomy of Exotic Higgs Decays in 2HDM*, *JHEP* **09** (2016) 093 [arXiv:1604.01406] [INSPIRE].

[13] ATLAS collaboration, *Search for a heavy Higgs boson decaying into a Z boson and another heavy Higgs boson in the $\ell\ell bb$ final state in pp collisions at $\sqrt{s} = 13$ TeV with the ATLAS detector*, *Phys. Lett.* **B 783** (2018) 392 [arXiv:1804.01126] [INSPIRE].

JHEP06(2019)031

[14] CMS collaboration, *Search for neutral resonances decaying into a Z boson and a pair of b jets or τ leptons*, *Phys. Lett.* **B 759** (2016) 369 [arXiv:1603.02991] [INSPIRE].

[15] ATLAS collaboration, *Search for heavy resonances decaying into a W or Z boson and a Higgs boson in final states with leptons and b-jets in 36 fb^{-1} of $\sqrt{s} = 13$ TeV pp collisions with the ATLAS detector*, *JHEP* **03** (2018) 174 [*Erratum ibid.* **11** (2018) 051] [arXiv:1712.06518] [INSPIRE].

[16] ATLAS collaboration, *Search for Higgs boson pair production in the $\gamma\gamma b\bar{b}$ final state with 13 TeV pp collision data collected by the ATLAS experiment*, *JHEP* **11** (2018) 040 [arXiv:1807.04873] [INSPIRE].

[17] CMS collaboration, *Search for Higgs boson pair production in the $\gamma\gamma b\bar{b}$ final state in pp collisions at $\sqrt{s} = 13$ TeV*, *Phys. Lett.* **B 788** (2019) 7 [arXiv:1806.00408] [INSPIRE].

[18] M. Benedikt et al., *Future Circular Collider*, CERN-ACC-2018-0058 (2018).

[19] T. Plehn, M. Spannowsky, M. Takeuchi and D. Zerwas, *Stop Reconstruction with Tagged Tops*, *JHEP* **10** (2010) 078 [arXiv:1006.2833] [INSPIRE].

[20] T. Plehn, M. Spannowsky and M. Takeuchi, *How to Improve Top Tagging*, *Phys. Rev.* **D 85** (2012) 034029 [arXiv:1111.5034] [INSPIRE].

[21] F. Kling, T. Plehn and M. Takeuchi, *Tagging single Tops*, *Phys. Rev.* **D 86** (2012) 094029 [arXiv:1207.4787] [INSPIRE].

[22] D.E. Kaplan, K. Rehermann, M.D. Schwartz and B. Tweedie, *Top Tagging: A Method for Identifying Boosted Hadronically Decaying Top Quarks*, *Phys. Rev. Lett.* **101** (2008) 142001 [arXiv:0806.0848] [INSPIRE].

[23] J. Thaler and K. Van Tilburg, *Maximizing Boosted Top Identification by Minimizing N-subjettiness*, *JHEP* **02** (2012) 093 [arXiv:1108.2701] [INSPIRE].

[24] G. Kasieczka, T. Plehn, M. Russell and T. Schell, *Deep-learning Top Taggers or The End of QCD?*, *JHEP* **05** (2017) 006 [arXiv:1701.08784] [INSPIRE].

[25] K. Kondo, *Dynamical Likelihood Method for Reconstruction of Events With Missing Momentum. 1: Method and Toy Models*, *J. Phys. Soc. Jap.* **57** (1988) 4126 [INSPIRE].

[26] J.S. Gainer, J. Lykken, K.T. Matchev, S. Mrenna and M. Park, *The Matrix Element Method: Past, Present and Future*, in *Proceedings, 2013 Community Summer Study on the Future of U.S. Particle Physics: Snowmass on the Mississippi (CSS2013)*, Minneapolis, MN, U.S.A., July 29–August 6, 2013 (2013) [arXiv:1307.3546] [INSPIRE].

[27] J. Brehmer, K. Cranmer, F. Kling and T. Plehn, *Better Higgs boson measurements through information geometry*, *Phys. Rev.* **D 95** (2017) 073002 [arXiv:1612.05261] [INSPIRE].

[28] J. Brehmer, F. Kling, T. Plehn and T.M.P. Tait, *Better Higgs-CP Tests Through Information Geometry*, *Phys. Rev.* **D 97** (2018) 095017 [arXiv:1712.02350] [INSPIRE].

[29] F. Kling, *Exotic Higgs Decays*, Ph.D. Thesis, Arizona U. (2016) [INSPIRE].

[30] A. Pyarelal, *Hidden Higgses and Dark Matter at Current and Future Colliders*, Ph.D. Thesis, Arizona U. (2017) [INSPIRE].

[31] B. Coleppa, F. Kling and S. Su, *Constraining Type II 2HDM in Light of LHC Higgs Searches*, *JHEP* **01** (2014) 161 [arXiv:1305.0002] [INSPIRE].

JHEP06(2019)031

[32] ATLAS and CMS collaborations, *Measurements of the Higgs boson production and decay rates and constraints on its couplings from a combined ATLAS and CMS analysis of the LHC pp collision data at* $\sqrt{s} = 7$ *and* 8 *TeV*, *JHEP* **08** (2016) 045 [arXiv:1606.02266] [INSPIRE].

[33] J.F. Gunion and H.E. Haber, *The CP conserving two Higgs doublet model: The Approach to the decoupling limit*, *Phys. Rev.* **D 67** (2003) 075019 [hep-ph/0207010] [INSPIRE].

[34] I.F. Ginzburg and I.P. Ivanov, *Tree-level unitarity constraints in the most general 2HDM*, *Phys. Rev.* **D 72** (2005) 115010 [hep-ph/0508020] [INSPIRE].

[35] J. Haller, A. Hoecker, R. Kogler, K. Mönig, T. Peiffer and J. Stelzer, *Update of the global electroweak fit and constraints on two-Higgs-doublet models*, *Eur. Phys. J.* **C 78** (2018) 675 [arXiv:1803.01853] [INSPIRE].

[36] HFLAV collaboration, *Averages of b-hadron, c-hadron and* τ*-lepton properties as of summer 2016*, *Eur. Phys. J.* **C 77** (2017) 895 [arXiv:1612.07233] [INSPIRE].

[37] M. Misiak and M. Steinhauser, *Weak radiative decays of the B meson and bounds on* $M_{H^\pm}$ *in the Two-Higgs-Doublet Model*, *Eur. Phys. J.* **C 77** (2017) 201 [arXiv:1702.04571] [INSPIRE].

[38] T. Han, T. Li, S. Su and L.-T. Wang, *Non-Decoupling MSSM Higgs Sector and Light Superpartners*, *JHEP* **11** (2013) 053 [arXiv:1306.3229] [INSPIRE].

[39] ALEPH, DELPHI, L3, OPAL and LEP collaborations, *Search for Charged Higgs bosons: Combined Results Using LEP Data*, *Eur. Phys. J.* **C 73** (2013) 2463 [arXiv:1301.6065] [INSPIRE].

[40] ALEPH, DELPHI, L3 and OPAL collaborations, LEP Working Group for Higgs Boson Searches, *Search for neutral MSSM Higgs bosons at LEP*, *Eur. Phys. J.* **C 47** (2006) 547 [hep-ex/0602042] [INSPIRE].

[41] ATLAS collaboration, *Search for charged Higgs bosons decaying into top and bottom quarks at* $\sqrt{s} = 13$ *TeV with the ATLAS detector*, *JHEP* **11** (2018) 085 [arXiv:1808.03599] [INSPIRE].

[42] ATLAS collaboration, *Search for charged Higgs bosons decaying via* $H^\pm \to \tau^\pm \nu_\tau$ *in the* τ*+jets and* τ*+lepton final states with* 36 fb^{-1} *of pp collision data recorded at* $\sqrt{s} = 13$ *TeV with the ATLAS experiment*, *JHEP* **09** (2018) 139 [arXiv:1807.07915] [INSPIRE].

[43] CMS collaboration, *Search for charged Higgs bosons with the* $H^\pm \to \tau^\pm \nu_\tau$ *decay channel in the fully hadronic final state at* $\sqrt{s} = 13$ *TeV*, CMS-PAS-HIG-16-031 (2016).

[44] A.G. Akeroyd et al., *Prospects for charged Higgs searches at the LHC*, *Eur. Phys. J.* **C 77** (2017) 276 [arXiv:1607.01320] [INSPIRE].

[45] R.V. Harlander, S. Liebler and H. Mantler, *SusHi: A program for the calculation of Higgs production in gluon fusion and bottom-quark annihilation in the Standard Model and the MSSM*, *Comput. Phys. Commun.* **184** (2013) 1605 [arXiv:1212.3249] [INSPIRE].

[46] R.V. Harlander and W.B. Kilgore, *Next-to-next-to-leading order Higgs production at hadron colliders*, *Phys. Rev. Lett.* **88** (2002) 201801 [hep-ph/0201206] [INSPIRE].

[47] R.V. Harlander and W.B. Kilgore, *Higgs boson production in bottom quark fusion at next-to-next-to leading order*, *Phys. Rev.* **D 68** (2003) 013001 [hep-ph/0304035] [INSPIRE].

[48] J. Hajer, A. Ismail, F. Kling, Y.-Y. Li, T. Liu and S. Su, *Searches for non-SM heavy Higgses at a* 100 *TeV pp collider*, *Int. J. Mod. Phys.* **A 30** (2015) 1544005 [INSPIRE].

JHEP06(2019)031

[49] W. Beenakker, R. Hopker and M. Spira, *PROSPINO: A Program for the production of supersymmetric particles in next-to-leading order QCD*, hep-ph/9611232 [INSPIRE].

[50] T. Plehn, *Charged Higgs boson production in bottom gluon fusion*, *Phys. Rev.* **D 67** (2003) 014018 [hep-ph/0206121] [INSPIRE].

[51] CMS collaboration, *Search for additional neutral MSSM Higgs bosons in the $\tau\tau$ final state in proton-proton collisions at $\sqrt{s} = 13$ TeV*, *JHEP* **09** (2018) 007 [arXiv:1803.06553] [INSPIRE].

[52] ATLAS collaboration, *Search for additional heavy neutral Higgs and gauge bosons in the ditau final state produced in 36 fb^{-1} of pp collisions at $\sqrt{s} = 13$ TeV with the ATLAS detector*, *JHEP* **01** (2018) 055 [arXiv:1709.07242] [INSPIRE].

[53] D. Dicus, A. Stange and S. Willenbrock, *Higgs decay to top quarks at hadron colliders*, *Phys. Lett.* **B 333** (1994) 126 [hep-ph/9404359] [INSPIRE].

[54] S. Jung, J. Song and Y.W. Yoon, *Dip or nothingness of a Higgs resonance from the interference with a complex phase*, *Phys. Rev.* **D 92** (2015) 055009 [arXiv:1505.00291] [INSPIRE].

[55] M. Carena and Z. Liu, *Challenges and opportunities for heavy scalar searches in the $t\bar{t}$ channel at the LHC*, *JHEP* **11** (2016) 159 [arXiv:1608.07282] [INSPIRE].

[56] ATLAS collaboration, *Search for Heavy Higgs Bosons A/H Decaying to a Top Quark Pair in pp Collisions at $\sqrt{s} = 8$ TeV with the ATLAS Detector*, *Phys. Rev. Lett.* **119** (2017) 191803 [arXiv:1707.06025] [INSPIRE].

[57] N. Craig, J. Hajer, Y.-Y. Li, T. Liu and H. Zhang, *Heavy Higgs bosons at low $\tan\beta$: from the LHC to 100 TeV*, *JHEP* **01** (2017) 018 [arXiv:1605.08744] [INSPIRE].

[58] J. Hajer, Y.-Y. Li, T. Liu and J.F.H. Shiu, *Heavy Higgs Bosons at 14 TeV and 100 TeV*, *JHEP* **11** (2015) 124 [arXiv:1504.07617] [INSPIRE].

[59] A. Aboubrahim and P. Nath, *Naturalness, the hyperbolic branch and prospects for the observation of charged Higgs bosons at high luminosity LHC and 27 TeV LHC*, *Phys. Rev.* **D 98** (2018) 095024 [arXiv:1810.12868] [INSPIRE].

[60] N. Craig, F. D'Eramo, P. Draper, S. Thomas and H. Zhang, *The Hunt for the Rest of the Higgs Bosons*, *JHEP* **06** (2015) 137 [arXiv:1504.04630] [INSPIRE].

[61] M. Czakon, P. Fiedler and A. Mitov, *Total Top-Quark Pair-Production Cross Section at Hadron Colliders Through $O(\alpha_S^4)$*, *Phys. Rev. Lett.* **110** (2013) 252004 [arXiv:1303.6254] [INSPIRE].

[62] M.L. Mangano et al., *Physics at a 100 TeV pp Collider: Standard Model Processes*, *CERN Yellow Rep.* (2017) 1 [arXiv:1607.01831] [INSPIRE].

[63] F. Febres Cordero, L. Reina and D. Wackeroth, *W- and Z-boson production with a massive bottom-quark pair at the Large Hadron Collider*, *Phys. Rev.* **D 80** (2009) 034015 [arXiv:0906.1923] [INSPIRE].

[64] J. Alwall et al., *The automated computation of tree-level and next-to-leading order differential cross sections and their matching to parton shower simulations*, *JHEP* **07** (2014) 079 [arXiv:1405.0301] [INSPIRE].

[65] T. Sjöstrand, S. Mrenna and P.Z. Skands, *PYTHIA 6.4 Physics and Manual*, *JHEP* **05** (2006) 026 [hep-ph/0603175] [INSPIRE].

JHEP06(2019)031

[66] T. Sjöstrand et al., *An Introduction to PYTHIA 8.2*, *Comput. Phys. Commun.* **191** (2015) 159 [arXiv:1410.3012] [INSPIRE].

[67] DELPHES 3 collaboration, *DELPHES 3, A modular framework for fast simulation of a generic collider experiment*, *JHEP* **02** (2014) 057 [arXiv:1307.6346] [INSPIRE].

[68] D. Eriksson, J. Rathsman and O. Stal, *2HDMC: Two-Higgs-Doublet Model Calculator Physics and Manual*, *Comput. Phys. Commun.* **181** (2010) 189 [arXiv:0902.0851] [INSPIRE].

[69] F. Cascioli et al., *ZZ production at hadron colliders in NNLO QCD*, *Phys. Lett.* **B 735** (2014) 311 [arXiv:1405.2219] [INSPIRE].

[70] CMS collaboration, *Top Tagging with New Approaches*, CMS-PAS-JME-15-002 (2016).

[71] ATLAS collaboration, *Differential top-antitop cross-section measurements as a function of observables constructed from final-state particles using pp collisions at* $\sqrt{s} = 7$ *TeV in the ATLAS detector*, *JHEP* **06** (2015) 100 [arXiv:1502.05923] [INSPIRE].

[72] J. Li, R. Patrick, P. Sharma and A.G. Williams, *Boosting the charged Higgs search prospects using jet substructure at the LHC*, *JHEP* **11** (2016) 164 [arXiv:1609.02645] [INSPIRE].

[73] R. Patrick, P. Sharma and A.G. Williams, *Triple top signal as a probe of charged Higgs in a 2HDM*, *Phys. Lett.* **B 780** (2018) 603 [arXiv:1710.08086] [INSPIRE].

[74] J. Alwall, M. Herquet, F. Maltoni, O. Mattelaer and T. Stelzer, *MadGraph 5: Going Beyond*, *JHEP* **06** (2011) 128 [arXiv:1106.0522] [INSPIRE].

[75] C. Degrande, *Automatic evaluation of UV and R2 terms for beyond the Standard Model Lagrangians: a proof-of-principle*, *Comput. Phys. Commun.* **197** (2015) 239 [arXiv:1406.3030] [INSPIRE].

[76] FCC-HH Working Group, *FCC Pythia + Delphes Analysis (Documentation)*, http://fccsw.web.cern.ch/fccsw/tutorials/fcc-tutorials/FccPythiaDelphes.html.

[77] H.-J. Yang, B.P. Roe and J. Zhu, *Studies of boosted decision trees for MiniBooNE particle identification*, *Nucl. Instrum. Meth.* **A 555** (2005) 370 [physics/0508045] [INSPIRE].

[78] A. Hocker et al., *TMVA — Toolkit for Multivariate Data Analysis*, PoS(ACAT)040 [physics/0703039] [INSPIRE].

[79] N. Kumar and S.P. Martin, *Vectorlike Leptons at the Large Hadron Collider*, *Phys. Rev.* **D 92** (2015) 115018 [arXiv:1510.03456] [INSPIRE].

[80] G. Cowan, *Two developments in tests for discovery: use of weighted Monte Carlo events and an improved measure*, *Progress on Statistical Issues in Searches*, SLAC, June 4–6, 2012.

[81] G. Cowan, K. Cranmer, E. Gross and O. Vitells, *Asymptotic formulae for likelihood-based tests of new physics*, *Eur. Phys. J.* **C 71** (2011) 1554 [*Erratum ibid.* **C 73** (2013) 2501] [arXiv:1007.1727] [INSPIRE].

[82] M. Backović and J. Juknevich, *TemplateTagger v1.0.0: A Template Matching Tool for Jet Substructure*, *Comput. Phys. Commun.* **185** (2014) 1322 [arXiv:1212.2978] [INSPIRE].

[83] T. Plehn and M. Spannowsky, *Top Tagging*, *J. Phys.* **G 39** (2012) 083001 [arXiv:1112.4441] [INSPIRE].

[84] G. Kasieczka, T. Plehn, T. Schell, T. Strebler and G.P. Salam, *Resonance Searches with an Updated Top Tagger*, *JHEP* **06** (2015) 203 [arXiv:1503.05921] [INSPIRE].

JHEP06(2019)031

[85] J. Pearkes, W. Fedorko, A. Lister and C. Gay, *Jet Constituents for Deep Neural Network Based Top Quark Tagging*, arXiv:1704.02124 [INSPIRE].

[86] Y.L. Dokshitzer, G.D. Leder, S. Moretti and B.R. Webber, *Better jet clustering algorithms*, *JHEP* **08** (1997) 001 [hep-ph/9707323] [INSPIRE].

[87] M. Cacciari, G.P. Salam and G. Soyez, *FastJet User Manual*, *Eur. Phys. J.* **C 72** (2012) 1896 [arXiv:1111.6097] [INSPIRE].

[88] A.J. Larkoski, S. Marzani, G. Soyez and J. Thaler, *Soft Drop*, *JHEP* **05** (2014) 146 [arXiv:1402.2657] [INSPIRE].

JHEP06(2019)031